Acta Palaeobotanica 66(1), 19–50, 2026
https://doi.org/10.35535/acpa-2026-0002

e-ISSN 2082-0259
ISSN 0001-6594

Floristic composition and palaeoclimate of the early Paleocene Highvale Mine Ardley Coal Zone Fossil Flora, Central Alberta, Canada

CHRISTOPHER K. WEST[1*], TAMMO REICHGELT[2] and GEORGIA L. HOFFMAN[3]

[1] Royal Tyrrell Museum of Palaeontology, Drumheller, Alberta, T0J 0Y6, Canada; e-mail: christopher.west@gov.ab.ca, ORCID: 0000-0003-1193-0986

[2] Department of Earth Sciences, University of Connecticut, Beach Hall, 354 Mansfield Rd #207, Storrs, CT 06269, USA; e-mail: tammo.reichgelt@uconn.edu, ORCID: 0000-0001-8652-5489

[3] G. Hoffman Consulting Services, 1914 5th St. SW, Calgary, Alberta T2S 2B3 Canada; e-mail: orontiophyllum@gmail.com, ORCID: 0000-0002-5560-9783

Received 18 September 2025; accepted for publication 7 January 2026

ABSTRACT. The early Paleocene was a time of dramatic ecological transformation following the Cretaceous–Paleogene (K–Pg) mass extinction. Although terrestrial recovery has been well-studied in the Western Interior of the United States, macrofloral records from early Paleocene Canada remain sparse. Here, we describe a diverse early Paleocene fossil plant assemblage from the Ardley Coal Zone of the Scollard Formation at the Highvale Coal Mine in Alberta. The flora includes 27 leaf, fruit, and seed taxa and is composed of ferns, conifers, and broadleaf angiosperms preserved in floodplain and swamp deposits lying about 14 m above the K–Pg boundary. We present new taxonomic descriptions alongside quantitative palaeoclimate reconstructions using leaf physiognomic and Nearest Living Relative methods. These estimates, synthesized via an ensemble approach, indicate that Highvale supported a warm-temperate (mean annual temperature of 9.6°C), humid forest (relative humidity at 76.8%) with moderate seasonality (driest month precipitation at 4 cm) and moderate net primary productivity (701 gC m^{-2} yr^{-1}). These results are compared to those from the broadly coeval Genesee and Ravenscrag fossil floras, which reflect a latitudinal climate gradient and localized environmental variation during the early Paleocene in western Canada.

KEYWORDS: Danian, Western Canada, K–Pg, Net Primary Productivity, palaeoenvironment

INTRODUCTION

The early Paleocene was a time of profound ecological and climatic transformation following the Cretaceous–Paleogene (K–Pg) mass extinction. Triggered by an asteroid impact on the Yucatán Peninsula (Alvarez et al., 1980; Hildebrand et al., 1991), the K–Pg event witnessed the global disruption of earth system processes through the injection of aerosols and soot into the atmosphere, leading to reduced ground-reaching insolation, a collapse of photosynthetic productivity, marine food web disruption, and short-term global cooling (Schulte et al., 2010; Vellekoop et al., 2014). These effects were catastrophic but relatively short-lived (i.e., decadal scale); atmospheric opacity decreased over a relatively short period, and marine ecosystems showed signs of rapid recovery (e.g. Vellekoop et al., 2014, 2021; Rosenberg et al., 2021; Morgan et al., 2022).

On land, the K–Pg mass extinction radically reshaped terrestrial ecosystems. Mammals diversified rapidly and replaced non-avian dinosaurs as the dominant terrestrial vertebrates, and angiosperms assumed ecological dominance over gymnosperms in most vegetation assemblages (e.g. Vajda and Bercovici,

* Corresponding author

Publisher: W. Szafer Institute of Botany, Polish Academy of Sciences

2014; Carvalho et al., 2021; Wilf et al., 2023). Terrestrial recovery has been widely studied through fossil plant assemblages, particularly pollen and spores, although macrofloral data remain comparatively underutilized (Wilf and Johnson, 2004; Stiles et al., 2020; Wilson Deibel et al., 2024). These palaeobotanical records indicate substantial turnover of plant taxa at the boundary and reduced floral diversity during the earliest Paleocene (Orth et al., 1981; Nichols et al., 1986; Wolfe and Upchurch, 1986, 1987; Sweet et al., 1990; Johnson, 1992; Sweet and Braman, 2001; Barclay et al., 2003; Stiles et al., 2020; Prebble et al., 2021).

In North America, post-extinction vegetation dynamics have been particularly well documented across the Western Interior of the United States, where extensive sedimentary basins preserve a rich record of floral turnover and ecological succession (e.g. Brown, 1962; Johnson et al., 1989; Johnson, 1992, 2002; Davies-Vollum, 1997; Wilf et al., 2023; Wilson Deibel et al., 2024). Early Paleocene floras from the Williston, Powder River, and Denver basins record an abrupt decline in diversity at the boundary, followed by the establishment of pioneer-dominated plant communities, including fern spikes and fast-growing angiosperms (Johnson, 1992; Nichols and Johnson, 2002). These macrofloral records reveal a heterogeneous landscape of recovery, where floristic composition and structural complexity varied in response to differences in local environmental gradients, sediment accumulation rates, and basin evolution.

Compared to the relatively well-known early Paleocene floras from the United States, macrofloral records from similarly aged strata in Canada remain scarce. In Alberta and Saskatchewan, only a few early Paleocene assemblages have been described in detail (e.g. Chandrasekharam, 1974; McIver and Basinger, 1993), limiting the potential for evaluating regional recovery patterns and their drivers.

The Scollard Formation in Alberta is one of the only sedimentary units in western Canada that preserves a stratigraphically continuous record across the K–Pg boundary; it includes fossil plant assemblages from both the terminal Cretaceous and early Paleocene. The Scollard also includes a series of thick coal seams known as the Ardley Coal Zone (ACZ) that extends across the west-central Alberta Plains (Gibson, 1977; Demchuk, 1990; Langenberg et al., 2007) (Fig. 1A). The K–Pg boundary has been identified at the base of the lowermost ACZ coal seam (Russell and Singh, 1978; Sweet, 1986), which suggests an earliest Paleocene age for the ACZ.

Fossil plants preserved in the mudstone beds of the ACZ provide a window into forest ecosystems during the earliest Paleocene. In this study, we describe the fossil flora from the top of the ACZ at the Highvale Coal Mine (Fig. 1A, B) and propose several new taxonomic combinations. We also present new quantitative palaeoclimate reconstructions for the Highvale ACZ flora, as well as updated climate estimates for the coeval, and nearby, Genesee flora (Fig. 1B). We compare these floras to each other and to the Ravenscrag Butte flora of southeastern Saskatchewan – the only other early Paleocene site in western Canada with comparable data – and evaluate regional patterns of climate and vegetation structure patterns that developed after the K–Pg extinction. This integrative approach contributes to refining our understanding of terrestrial ecosystem recovery and early Paleocene forest dynamics following the most recent mass extinction.

MATERIALS AND METHODS

LOCALITY

The fossils described here were collected at the Highvale Coal Mine, about 70 km west of Edmonton in west-central Alberta, Canada (53°29′N, 114°34′W) (Fig. 1A). Highvale was an open-pit mine that produced subbituminous coal from the ACZ between 1970 and 2021. Fossil collection took place between 1977 and 1979 by groups from the University of Alberta that included W.S. Stewart, J.F. Basinger, R.A. Stockey, and D.W. Wighton. During that time, the mine was producing from Pits 1 and 2 (B. Lyons, pers. com. 2025) (Fig. 1B). The coal zone (Seams 1 to 6) was about 14 m thick in that area (Demchuk, 1992). The fossils came from a layer of grey mudstone that remained on top of the uppermost coal seam (Seam 1, Fig. 2A) after overburden had been removed to allow coal extraction (J.F. Basinger, pers. com. 2024). The fossiliferous layer is estimated to have been about 30 cm thick or less (B. Lyons, pers. com. 2025). Fossils were collected by prying out blocks of mudstone, which were then split along the bedding plane using hand tools. These fossils have not been the subject of any previous work or study since their collection.

The Highvale ACZ flora is compared with the Genesee (Chandrasekharam, 1974) and Ravenscrag Butte (McIver and Basinger, 1993) floras, which are of similar early Paleocene age. The Genesee site (53°21′N, 114°24′W), like the Highvale ACZ, is part of the upper Scollard Formation and lies about 22 km southeast of

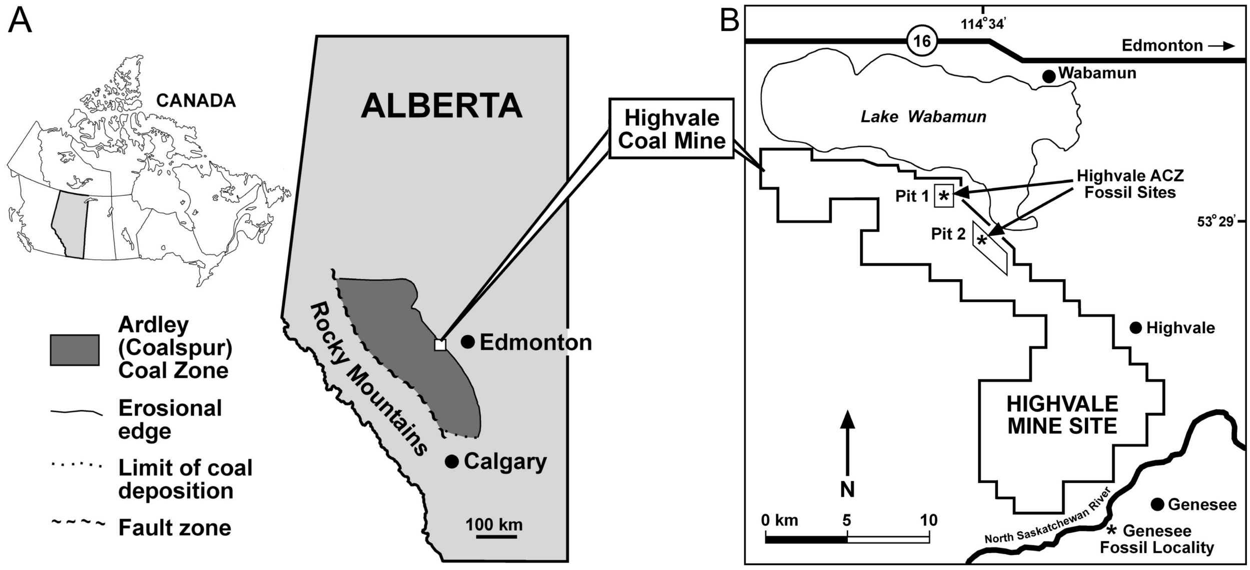

Figure 1. **A**. Simplified map of Alberta, Canada, showing the location of the Highvale Coal Mine; **B**. Map of the Highvale Coal Mine showing the location of the Highvale ACZ fossil sites and the Genesee fossil locality. Modified from Demchuk and Hills (1991)

the Highvale ACZ fossil site (Fig. 1B). Ravenscrag Butte (49°30.4′N, 109°1.2′W), part of the Frenchman Formation, is located in southeastern Saskatchewan, roughly 575 km southeast of the Highvale ACZ fossil site.

PRESERVATION AND STUDY

The Highvale ACZ plant fossils are preserved as carbonaceous compressions on grey carbonaceous, calcareous, and silty mudstone. Specimens were photographed using a Nikon D3200 DSLR camera fitted with a Nikon AF-S Micro NIKKOR 40 mm or AF-S NIKKOR 18–55 mm lens. They are accessioned into the University of Alberta Paleobotanical Collection (UAPC-ALTA) in Edmonton, Alberta, Canada.

GEOLOGICAL BACKGROUND

REGIONAL STRATIGRAPHY

The ACZ of the western Alberta plains is correlative with the Coalspur Coal Zone in the foothills of the Canadian Rockies to the west, where it is terminated by faulting. The coal zone thins southward until it pinches out entirely north of Calgary (Richardson et al., 1988; Jerzykiewicz, 1997; Langenberg et al., 2007) (Fig. 1A).

The ACZ is part of the Scollard Formation, a sequence of alluvial plain sediments that was deposited in west-central Alberta during the late Maastrichtian to early Danian. The Scollard is informally divided into a lower, late Maastrichtian member and an upper, early Paleocene (Danian) member (Demchuk, 1990; Demchuk and Hills, 1991), with the ACZ at the base of the upper member (Fig. 2A). The K–Pg boundary has been documented at the base of the lowermost coal seam of the ACZ (Russell and Singh, 1978; Sweet, 1986), indicating its earliest Paleocene age.

The Scollard Formation is overlain by the Selandian to Thanetian Paskapoo Formation (Gibson, 1977; Demchuk and Hills, 1991) or, in some areas, by unconsolidated Quaternary sediments, as was the case at the fossil site. In Saskatchewan, the lower Scollard Formation is equivalent to the Frenchman Formation, whereas the upper Scollard is correlative with the lower Ravenscrag Formation (Fig. 2B).

At the Highvale Mine, the ACZ is subdivided into six coal seams, designated Seams 1 through 6 in descending order (Fig. 2A) (for seam correlations and nomenclature used in other parts of Alberta, see Langenberg et al., 2007). In the area of active mining at the time of fossil collection (Pits 1 and 2; Fig. 1B), the ACZ was approximately 14 meters thick and included all six seams (Demchuk, 1992). The interseam strata consisted primarily of grey carbonaceous mudstones and shales with abundant fossil root traces (Demchuk et al., 1993), as did the immediately overlying mudstones that yielded the fossil flora described herein (J.F. Basinger, pers. comm. 2024).

AGE OF THE FLORA

In the area where the fossils were collected (Pits 1 and 2, Fig. 1B) the ACZ coal sequence (Seams 1 to 6) was about 14 m thick (Demchuk, 1992: figs 1.2, 1.5, 1.6), and the fossiliferous bed was estimated to lie about 30 cm

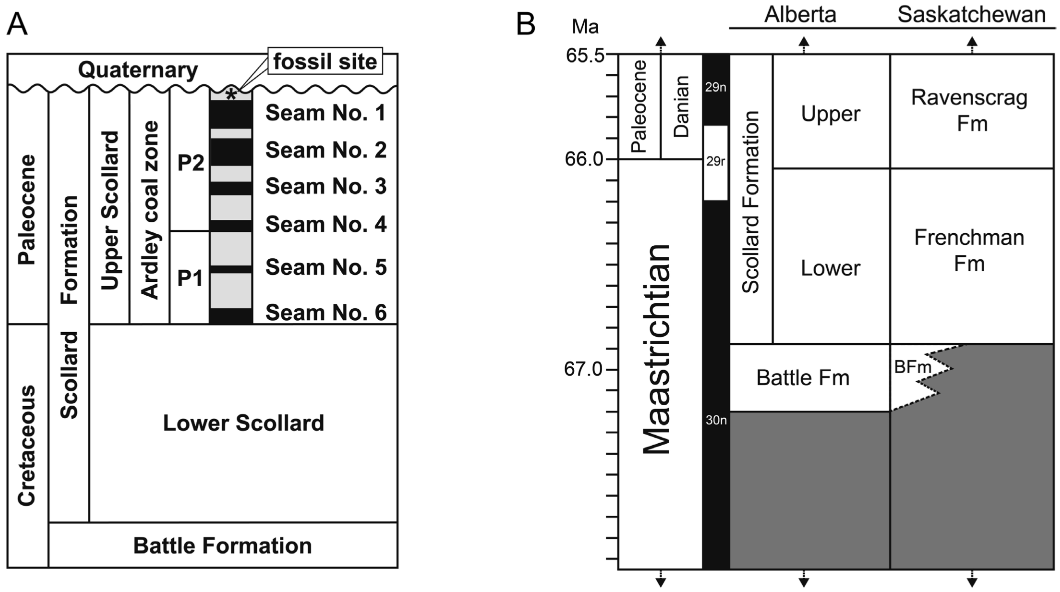

Figure 2. Simplified stratigraphic charts. **A**. Simplified stratigraphy of the Scollard Formation at the Highvale Coal Mine, indicating the stratigraphic position of the Ardley Coal Zone fossil flora. P1 = Pollen Zone 1 and P2 = Pollen Zone 2. Modified from Demchuk and Hills (1991); **B**. Simplified regional correlations between the Scollard Formation in Alberta, and the Ravenscrag Formation in Saskatchewan (modified from West et al. 2021)

above the top of Seam 1 (B. Lyons, pers. com. 2025) (Fig. 2A). Palynostratigraphic studies at the mine established that the K–Pg boundary lies at the base of Seam 6 (Sweet, 1986; Demchuk, 1992), therefore the fossiliferous bed would have sat roughly 14.3 m above the K–Pg boundary. The lower approximately 3.5 m of the ACZ (the portion below Seam 4; Fig. 2A) lay in the *Wodehouseia fimbriata* (P1) pollen zone of Demchuk (1987, 1990). Seam 4 and above was assigned to the *Momipites wyomingensis* (P2) zone (Demchuk, 1992).

Radiometric U–Pb dating of zircons from a bentonite bed near the top the Arbour Seam in the Coalspur Coal Zone yielded an age of 63.9 ± 0.5 Ma (Langenberg et al., 2007). The Arbour Seam is correlative with Seam 4 and above in the ACZ: both sit within the *Momipites wyomingensis* (P2) zone (Langenberg et al., 2007). Accordingly, we interpret the fossil-bearing beds of the Highvale ACZ to have been deposited around 63.9 Ma, indicating that peat accumulation in the ACZ persisted for at least two million years following the K–Pg boundary.

The Genesee flora is similar in age to the Highvale ACZ flora. The plant fossils at Genesee occur in light-coloured siltstone and were originally estimated to sit up to 30 m above the ACZ; however, the strata in the Genesee area are disturbed by glacial deformation and slumping, making the stratigraphic position of the fossiliferous beds difficult to interpret (Chandrasekharam, 1974). Later, Stockey et al. (2014) assigned the Genesee flora to Pollen Zone P1 of Nichols and Ott (1978), which correlates with the *Wodehouseia fimbriata* or P1 zone of Demchuk (1990). This is further confirmed by the presence of *W. fimbriata* pollen from samples taken from the Genesee fossil beds (D. Braman, pers. comm. 2025). Although both the Genesee and Highvale floras date to the early Paleocene, the presence of *W. fimbriata* suggests the Genesee flora is slightly older.

PALAEOCLIMATE

Fossil plants are excellent palaeoclimate proxies. This is because fossil plants, much like their modern equivalents, are in constant interaction with their surrounding environment, and as a consequence of their sessile lifestyle, they reflect the external conditions at the time of their growth. Leaves especially must have an optimal morphology to photosynthesize most efficiently, and thus leaf morphology (physiognomy) tends to be an expression of a plant's growth environment. Leaf traits of woody 'dicots' (herein 'dicots' indicates non-monocot angiosperms, including magnoliids) respond plastically to climate changes and many traits are evolutionarily convergent across broad phylogenetic lines (e.g. Royer et al., 2009; Yang et al., 2015; Spicer et al., 2021). Thus, 'dicot' fossil leaf physiognomy can be used for palaeoclimate reconstruction. The backbone for these methods is large datasets of modern leaf morphology and associated local climates (Yang et al., 2015). These physiognomic methods are applicable only to 'dicot' taxa. To reconstruct the palaeoclimate of the Highvale ACZ fossil flora, we applied three leaf physiognomic methods: Climate Leaf Analysis Multivariate Program (CLAMP), Leaf Area Analysis (LAA), and Leaf Margin Analysis (LMA). The palaeoclimate for the Genesee fossil flora was also reconstructed using CLAMP, and LAA values were taken from a previous study (Greenwood and West, 2017). CLAMP, LMA, and LAA data for Highvale are provided in the supplementary materials (CLAMP – Supplementary File 1[1] and 2[2]; LMA and LAA – Supplementary File 3[3]).

CLAMP

The Climate Leaf Analysis Multivariate Program (CLAMP) is a statistical approach employing canonical correspondence analysis (CCA) to reconstruct palaeoclimate. CLAMP relies on modern 'dicot' leaf physiognomic characteristics observed under known climate conditions. These leaf traits include a wide array of attributes: leaf size, lamina shape, presence or absence of lobes, margin characteristics, shapes of leaf apex and base, and length-width ratios. Fossil leaf assemblages are evaluated using the same criteria, and palaeoclimates are inferred by locating the nearest analogues in multidimensional space with CCA and calibrated using datasets of modern vegetation and climate (Wolfe, 1993; Spicer, 2008; Yang et al., 2011; Spicer et al., 2021).

Utilizing the Physg3brcAZ calibration dataset (Yang et al., 2011, 2015), we reconstruct the following variables for the ACZ fossil flora using CLAMP: mean annual temperature (MAT), warmest and coldest quarter temperature (WQT and CQT), mean annual precipitation (MAP), wettest month (WMP), driest month (DMP), relative humidity (RH), and net primary productivity (NPP). The climate variables were sourced from WORLDCLIM (Fick and Hijmans, 2017) and applied to the CLAMP modern calibration dataset (Yang et al., 2015; Reichgelt et al., 2022).

Net Primary Productivity (NPP) of a fossil locality can be estimated using the CLAMP calibration datasets. For this study, NPP values for the Physg3brcAZ calibration sites were derived from MODIS (Running et al., 2015). Previous work has shown leaf size to be a reliable predictor of ecosystem NPP (Li et al., 2020). However, rather than calculating NPP independently from leaf size, NPP was incorporated directly into the CLAMP CCA, following the approach outlined in Reichgelt and West (2025). Thus, NPP behaves like any other CLAMP variable, where the CCA identifies the most similar NPP values in multivariate physiognomic space based on multiple leaf characteristics and their associations with other environmental parameters. Importantly, this is the same CCA analysis that produces the reconstructed WORLDCLIM climatic variables discussed above; NPP is not generated through a separate analysis. As for the CLAMP WORDCLIM variables, NPP for the fossil sites were reconstructed by correlating CCA vector scores of ecosystem-level NPP in the Physg3brcAZ calibration dataset with the CCA vector scores obtained for the fossil assemblages. Regression functions derived from the calibration dataset were then used to predict NPP at the fossil sites, while error is calculated using the residual values of NPP from the calibration dataset. NPP is square rooted in the calibration dataset, to account for the relatively large NPP range in productive biomes, such as rainforests, relative to low NPP range in less productive biomes, such as tundra and desert (Reichgelt and West, 2025).

NPP and the variables derived from WORLDCLIM for the Highvale ACZ and Genesee fossil flora were reconstructed following standard CLAMP methodology (Wolfe, 1993; Spicer, 2008; Yang et al., 2011; Spicer et al., 2021) and executed in R using CCA in the *vegan* package (R Core Team, 2024; Oksanen et al., 2025).

Leaf Margin Analysis

Leaf Margin Analysis (LMA) is based on the linear correlation between MAT and the proportion of leaf taxa with smooth (untoothed) margins, referred to as the leaf margin proportion (LMP). A higher LMP typically indicates warmer climatic conditions (Wilf, 1997). Equation 1 represents the standard LMA regression (Wing and Greenwood, 1993). The standard error for MAT estimated by Equation 1 is calculated using the number of morphotypes identified within the fossil

[1] Supplementary File 1: Highvale Mine Flora CLAMP.

[2] Supplementary File 2: Genesee Highvale CLAMP CCA Report.

[3] Supplementary File 3: Highvale NLR Data.

assemblage (Equation 2; Wilf, 1997), where r denotes the number of morphotypes.

$$MAT = 1.141 + (30.6 \times LMP) \quad \text{(Eq. 1)}$$

$$\sigma MAT = 30.6\sqrt{(1 - LMP)/r} \quad \text{(Eq. 2)}$$

Leaf Area Analysis

Leaf Area Analysis (LAA) estimates MAP by utilizing the natural logarithm of the mean leaf area (MlnA) within a vegetation assemblage (Wilf et al., 1998). Leaf areas were determined by measuring leaves in photographs with ImageJ (Schneider et al., 2012). MAP values were estimated using the linear regression equation (Equation 3) proposed by Wilf et al. (1998).

$$\ln(MAP) = 0.768 + (0.548 \times MlnA) \quad \text{(Eq. 3)}$$

Standard errors for this equation were calculated using conventional linear regression techniques. However, because the regression models were originally developed using the natural logarithm (ln) of the dependent variable, back-transforming the results into the original (non-logarithmic) scale introduces asymmetry in the associated errors (Wilf et al., 1998).

Nearest Living Relative

Nearest Living Relative (NLR) analysis was employed to derive palaeoclimatic information from fossil assemblages based on the modern-day distribution of NLRs associated with the fossil flora. In this study, NLR analysis was conducted by calculating highest probability density intervals (e.g. Willard et al., 2019; West et al., 2020). Geodetic coordinates for each NLR were obtained from the Global Biodiversity Information Facility (https://www.gbif.org/). Exotic occurrences (i.e. taxa found outside their native range) were removed from the dataset. To mitigate regional overrepresentation in areas with extensive plant collections, the datasets were randomly resampled (see West et al., 2020). NLR data for Highvale and Genesee are provided in the supplementary materials (Supplementary File 4[4]).

Climatic envelopes for MAT, WQT, CQT, MAP and DMP were generated for each plant group by cross-referencing the filtered geodetic coordinates with gridded climate maps using the *dismo* package in R (Hijmans et al., 2005). A random set of >800,000 unique combinations of MAT, WQT, CQT, MAP and DMP was then generated. For each climatic variable (c), the likelihood (f) of the taxa (t) in the Highvale ACZ and Genesee fossil floras occurring under those conditions was calculated using the means (μ) and standard deviations (σ) of their modern distributions (Equation 4).

$$f(t_n) = \prod_{i=1}^{5} \left(1/\sqrt{2\sigma_c^2 \times \pi}\right) \times e^{x_c - \mu_c/2\sigma_c^2} \quad \text{(Eq. 4)}$$

Here, x_c represents a specific value of MAT, WQT, CQT, MAP and DMP that generates a unique combination, for which the likelihood of the taxa existing in that climate is calculated. The combined likelihood for the total number of taxa (n) was then determined using Equation 5.

$$f(z) = \prod_{i=1}^{n} f(t_n) \quad \text{(Eq. 5)}$$

The combination of MAT, WQT, CQT, MAP and DMP with the highest $f(z)$ is considered the value most representative of the assemblage, whereas the 95% confidence interval is the maximum range of these climatic variables, with $f(z) \geq 5\%$ the maximum $f(z)$.

Ensemble Method

Although using both leaf physiognomic and NLR methods allows for climate reconstruction from multiple independent proxies, their results are not always consistent, leading to ongoing debates regarding their accuracy and validity. Often, methodological preferences are influenced by perceived limitations specific to each approach. To overcome these issues, we employ the ensemble method, which integrates multiple proxy reconstructions into a unified consensus without preferential weighting (Lowe et al., 2018; West et al., 2020, 2021; Reichgelt et al., 2022). This ensemble strategy is currently regarded as producing the most parsimonious palaeobotanical climate reconstructions (Hollis et al., 2019; West et al., 2020).

The ensemble approach helps identify discrepancies among proxy reconstructions, but also significantly reduces uncertainty by producing probability density intervals that objectively reflect the inherent variability of proxy estimates (West et al., 2020). Additionally, it improves reconstruction reliability by explicitly incorporating and propagating uncertainties from each individual method, resulting in a robust consensus estimate (West et al., 2020; Reichgelt et al., 2022).

[4] Supplementary File 4: Highvale NLR Data.

In this study, we apply the ensemble method to derive the most parsimonious climate reconstructions from both leaf physiognomic and NLR results. Ensemble estimates for MAT, MAP, WQT, CQT and DMP were obtained through bootstrapping across all proxies, i.e. MAT from CLAMP, NLR, and LMA; MAP from CLAMP, NLR, and LAA; and the remainder from CLAMP and NLR. Specifically, each proxy reconstruction was resampled using Monte Carlo simulations (n = 1000) based on the means and standard deviations derived from individual proxies. These resampled datasets were then combined, generating ensemble means and associated standard deviations. For precipitation estimates (MAP and DMP), log-transformed values were resampled to account for asymmetric errors.

Closest Climatic Analogue

In order to quantitatively identify the closest climatic analogue in the modern world, we used the Closest Climatic Analogue technique (West et al., 2021, 2024). This approach takes ~250,000 randomly generated geodetic coordinates and obtains modern climate parameters (MAT, MAP, WQT, CQT and DMP) from WORLDCLIM using the *dismo* package in R (Hijmans et al., 2005). These climatic parameters ($x_{j,k}$) are normalized to Z scores ($Z_{j,k}$) using the mean (μ_j) and standard deviation (σ_j) for each climatic variable, so that variance is comparable between different climatic variables (j) across all locations (k) (Equation 6).

$$Z_{j,k} = \frac{x_{j,k} - \mu_j}{\sigma_j} \qquad \text{(Eq. 6)}$$

The $Z_{j,k}$ score is then also calculated for the reconstructed palaeoclimate of the fossil site. The dissimilarity for each modern site to the fossil site was then calculated, by summing the distances in $Z_{j,k}$ scores from the modern site (Z_X) to the fossil site (Z_F) (Equation 7).

$$d(X,F) = \log \sum_{n=1}^{5} (Z_X - Z_F)^2 \qquad \text{(Eq. 7)}$$

Inverse Distance Weighting (IDW) $d(X, F)$ values in ArcGIS Pro 3.1.0 (ESRI, 2023) were then used to create a map that indicates where in the world the most similar climates to the fossil site are. IDW was run with the number of nearest points to determine the cell value set at 12, and a maximum distance of 0.5°.

PALAEOENVIRONMENT

Climate data can help infer the type of vegetation present at a site. Whittaker (1962; 1975) developed global biome classifications based on mean annual temperature (MAT) and mean annual precipitation (MAP). Importantly, MAT and MAP alone do not capture the full range of vegetation variation observed in fossil leaf assemblages; however, Whittaker's biome framework remains useful for broadly characterizing potential vegetation types (e.g. Flynn and Peppe, 2019; West et al., 2020; Reichgelt and West, 2025). This is particularly relevant in terrestrial settings where the macroclimate differed substantially from that of today, such as in high-latitude regions that supported warm-adapted vegetation during ancient greenhouse intervals (West et al., 2020). In this study, Whittaker biomes were plotted using the *plotbiomes* R package (Ştefan and Levin, 2018).

RESULTS

SYSTEMATIC PALAEONTOLOGY

Broadleaf 'dicot' (non-monocot angiosperms, including magnoliids) fossils were described using the standardized morphological criteria and terminology of Ellis et al. (2009). No similar standardized system exists for fossil gymnosperms, ferns, monocot leaves, seeds, or fruits, therefore, descriptions followed standard practice for botanical descriptions, drawing on comparative morphology and previously established taxonomic literature. Twenty-seven plant taxa are described (Table 1), including 1 horsetail, 1 fern, 2 conifers, 18 angiosperm leaves, 4 reproductive structures, and roots and stem casts.

POLYPODIOPSIDA

Order EQUISETALES
DC. ex Bercht. et J. Presl. 1820

Family EQUISETACEAE Michx. ex DC 1804

Genus *Equisetum* L. 1753

Equisetum sp.

Fig. 3A

Specimens examined. S7725, S7728, S7769.

Table 1. Systematic list of the ACZ fossil flora described from the Highvale Coal Mine, Alberta, Canada

Polypodiopsida	Equisetales DC. ex Bercht. et J. Presl. 1820	Equisetaceae Michx. ex DC 1804	*Equisetum* L. 1753	
	Osmundales Link 1833	Osmundaceae Martinov 1820	*Osmunda* L. 1753	*Osmunda macrophylla* Penh. 1908
Pinopsida	Cupressales Link 1829	Cupressaceae Gray 1821	*Metasequoia* Hu et W.C.Cheng 1948	*Metasequoia occidentalis* (Newb. 1863) R.W.Chaney 1951
			Glyptostrobus Endl. 1847	*Glyptostrobus nordenskioldii* (Heer 1870) R.W.Br. 1962
Angiosperms	Proteales Juss. ex Bercht. et J. Presl. 1820	Platanaceae T. Lestib 1826	*Platanites* Forbes 1851	
	Trochodendrales Takht. ex Cronquist 1981	Trochodendraceae Eichler 1865	*Nordenskioeldia* Heer 1870	*Nordenskioeldia borealis* Heer emend. P.R Crane, Manchester et Dilcher 1991
			Zizyphoides Seward et V.M.Conway 1935 emend. Zolina, Manchester et Golovn. 2021	*Zizyphoides flabella* (Newb. 1863) P.R.Crane, Manchester et Dilcher 1991
	Saxifragales Bercht. et J. Presl. 1820	Cercidiphyllaceae Engl. 1907	*Archeampelos* McIver et Basinger 1993	*Archeampelos lobocrenata* (Lesq. 1873) Doweld 2016
			Trochodendroides E.W.Berry 1922	*Trochodendroides genesevianum* (Chandrasekharam 1974) C.K.West, Reichgelt et G.L.Hoffman comb. nov. *Trochodendroides flexuosa* (Hollick 1936) C.K.West, Reichgelt et G.L.Hoffman comb. nov. *Trochodendroides cuneatum* (Newb. 1898) C.K.West, Reichgelt et G.L.Hoffman comb. nov.
			Jenkinsella E.Reid et M.Chandler 1933	*Jenkinsella arctica* (Heer 1870) W.A.Bell 1949
	Fagales Engl. 1892	Betulaceae Gray 1822	*Craspedodromophyllum* P.R.Crane 1981	*Craspedodromophyllum* cf. *C. malmgrenii* (Heer 1868) Golovneva 2002
	Caryophyllales Juss. ex Bercht. et J. Presl. 1820	Polygonaceae Juss. 1789	*Paranymphaea* E.W.Berry 1935	*Paranymphaea crassifolia* (Newb. 1868) E.W.Berry 1935
	Cornales Link 1829	Nyssaceae Juss. Ex Dumort. 1829	*Browniea* Manchester et L.Hickey 2007	*Browniea serrata* (Newb. 1868) Manchester et L.Hickey 2007
Incertae Sedis				cf. *Pterospermites* Heer 1859 Unidentified leaf 1 Unidentified leaf 2 Unidentified leaf 3 Unidentified leaf 4 Unidentified leaf 5 Unidentified leaf 6 Unidentified leaf 7 Unidentified leaf 8 Unidentified seeds Unidentified roots Unidentified stem casts

D e s c r i p t i o n. Leaves, fused into collars, 14–16 leaves per collar; unfused portions of leaves up to 4 mm long; apex acute or acuminate, appear appressed. Axes up to ~7 mm in diameter, grooved and ridged longitudinally. Rhizomes or stems branching at nodes, ~14 mm wide, up to 148 mm long; adventitious roots present; roots 10–17 mm long.

R e m a r k s. The remains recovered from Highvale ACZ are identifiable as *Equisetum* sp. based on the presence of characteristic leaf collars, a diagnostic feature of the genus. However, given the limited quantity of material available, we refrain from making any more specific taxonomic assignment at this time.

Order OSMUNDALES Link 1833

Family OSMUNDACEAE Martinov 1820

Genus *Osmunda* L. 1753

Osmunda macrophylla Penh. 1908

Fig. 3B

S p e c i m e n s e x a m i n e d. S7809, S7812.

D e s c r i p t i o n. Pinna up to 44 mm long but incomplete, up to 20 mm wide, rachis 0.3–0.6 mm wide. Pinnules alternate, narrow-ovate, up to 15 mm long, up to 5.5 mm wide;

apex obtuse; base truncate; pinnule margin entire; pinnules attached to rachis by a short stalk but appear sessile. Venation open dichotomous; midvein stout, continuous toward apex; secondary veins dichotomize once or twice before reaching margin.

Remarks. The size, shape, and open dichotomous venation pattern of these pinnules are consistent with those of other reported occurrences of *O. macrophylla* from the Paleocene of Alberta, Saskatchewan, North Dakota and Montana (Penhallow, 1908; Bell, 1949; Brown, 1962; McIver and Basinger, 1993). The presence of the palynomorph *Osmundacidites* in pollen assemblages from the Highvale ACZ coal seams (Demchuk, 1992) tends to support its affinity to extant *Osmunda*. However, no fertile material is known for *O. macrophylla* (e.g. Brown, 1962), and its assignment to the extant genus therefore remains uncertain.

PINOPSIDA

Order CUPRESSALES Link 1829

Family CUPRESSACEAE Gray 1821

Genus *Metasequoia* Hu et W.C.Cheng 1948

Metasequoia occidentalis
(Newb. 1863) R.W.Chaney 1951

Fig. 3E, F

Specimens examined. S5459, S7726, S7736, S7785, S7805, S7820.

Description. Leafy branches up to 126 mm long, oppositely branched, forming flat sprays of branchlets, branchlets up to 64 mm long. Leaves opposite, decussate; leaves distantly spaced on branch axis, up to 10 mm apart, leaves closely clustered on branchlets; midvein distinct; leaf shape ovate to linear, 5–13 mm long, 0.75–1.2 mm wide; leaf apex blunt to rounded or rarely acute, base symmetrical, petiole short, attachment decurrent, twisted on facial leaves. Seed cones 13–26 mm long, 11–24 mm wide, globose or ovoid, found unattached or born terminally on long bare stalks up to 113 mm long; cone scale complex 5.5–8.3 mm long, peltate, decussate.

Remarks. The leafy shoots and seed cones are comparable to other examples of *Metasequoia occidentalis* from North America (Chaney, 1951; Chandrasekharam, 1974; Christophel, 1976; Hickey, 1977; McIver and Basinger, 1993; West et al., 2019). The leafy shoots have opposite and decussate leaf phyllotaxy, and the seed cones show a decussate cone scale complex typical for both *M. occidentalis* and the extant *M. glyptostroboides* Hu et W.C.Cheng (Chaney, 1951; Brown, 1962; McIver and Basinger, 1993; Liu et al., 1999; Stockey et al., 2001; Jin et al., 2012; West et al., 2019). *M. occidentalis* is a well-documented and widespread component of Paleocene-aged deposits in Alberta (e.g. Chandrasekharam, 1974; Christophel, 1976; Hoffman and Stockey, 1999), frequently occurring in macrofossil assemblages, and taxodiaceous palynomorphs attributed to the genus, such as *Metasequoiapollenites* are common in palynological records and are present in pollen assemblages from the Highvale ACZ coal seams (Demchuk, 1992). The consistent presence of *Metasequoia* across multiple sites suggests it was a dominant element of lowland wetland and riparian forest ecosystems during the early Paleogene.

Genus *Glyptostrobus* Endl. 1847

Glyptostrobus nordenskioldii
(Heer 1870) R.W.Br. 1962

Fig. 3C, D, G

Specimens examined. S6847, S6856, S6869, S7738, S7740, S7746, S7775, S7777.

Description. Branches up to 87 mm long, branchlets up to 39 mm long; leaves polymorphic, alternate, helical, cupressoid, crypto-cupressoid, crypto-taxodioid. Cupressoid leaves 1.3–1.8 mm long, appressed along stem, awl- or hook-shaped or straight or slightly curving, apex acute. Crypto-cupressoid leaves 2.2–3.5 mm long, may appear twisted, decurrent at base; leaves straight or curved apically. Crypto-taxodioid leaves 7.6–9.1 mm long, flattened, apices blunt to sharp. Pollen cones alternate, terminal, orbicular to ovate in shape, borne on branches with cupressoid leaves, 1.5–2.2 mm long, 2–2.5 mm wide.

Remarks. Described from numerous specimens of sterile foliage and pollen cones, the material is consistent with fossil material previously described as *Glyptostrobus nordenskioldii* from Alberta (Christophel, 1976), and

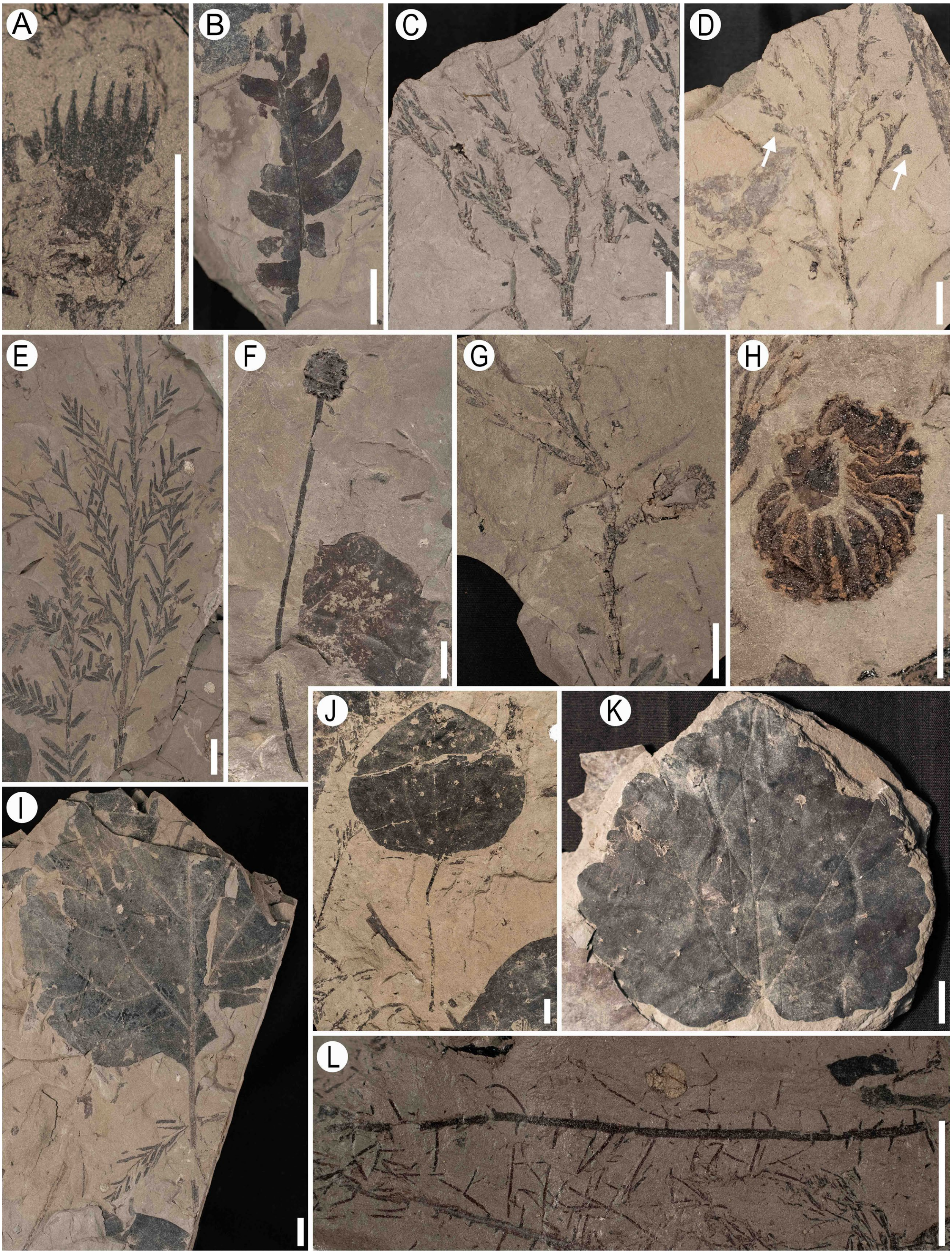

Figure 3. Fossils of the Highvale ACZ flora. **A**. *Equisetum* sp., leaf collar, S7769; **B**. *Osmunda macrophylla*, frond, S7812; **C**. *Glyptostrobus nordenskioldii*, leafy branch, S6856; **D**. *Glyptostrobus nordenskioldii*, leafy branch with arrows pointing at cones, S7738; **E**. *Metasequoia occidentalis*, leafy branch, S7820; **F**. *Metasequoia occidentalis*, cone, S7736; **G**. *Glyptostrobus nordenskioldii*, leafy branch with cone, S7777; **H**. *Nordenskioeldia borealis*, fruit, S10543; **I**. *Platanites* sp., leaf, S7756; **J**. *Zizyphoides flabella*, leaf, S7721; **K**. *Archeampelos lobocrenata*, leaf, S7741; **L**. Unidentified roots, S7731. Scale bars = 1 cm

elsewhere in North America (Brown, 1962, Hickey, 1977; McIver and Basinger, 1993; West et al., 2019). Although no seed cones are formally described, a single specimen appears to represent a seed cone (Fig. 3G), lending further evidence for the taxonomic assignment. Given the similarity between these specimens and those described from the Paleocene Smoky Tower locality in Alberta (Christophel, 1976), and the early Paleocene Ravenscrag flora in Saskatchewan (McIver and Basinger, 1993), we assign them to the same taxon. *Glyptostrobus nordenskioldii* is a common and widely distributed conifer species in Paleogene fossil floras of the Northern Hemisphere, including Alberta (Christophel, 1976; McIver and Basinger, 1993; West et al., 2019), and the cupressaceous palynomorph *Taxodiaceaepollenites hiatus*, which may have been produced by *G. nordenskioldii*, is abundant in pollen assemblages from the Highvale ACZ coal seams (Demchuk, 1992). *G. nordenskioldii* is typically associated with swampy or riparian environments. Its frequent co-occurrence with *Metasequoia* and other wetland taxa suggests that it played a significant ecological role in the composition of Paleocene lowland forest ecosystems.

ANGIOSPERMAE

Order PROTEALES
Juss. ex Bercht. et J. Presl. 1820

Family PLATANACEAE T.Lestib 1826

Genus *Platanites* Forbes 1851

Platanites sp.

Fig. 3I

Specimens examined. S5484, S6859, S6871, S7756, S7790, S7814.

Description. Leaf mesophyllous, petiolate, leaf attachment marginal; base angle obtuse, base shape rounded, decurrent, or cuneate. Leaf margin serrately crenate to serrate, with 1 order of teeth, 2 teeth per cm, tooth shape convex/convex to concave/convex, sinus rounded. Primary venation basal actinodromous to suprabasal actinodromous, with 3 basal veins, primary vein 1.29–1.47 mm thick, lateral primary veins 0.99–1.37 mm thick; simple agrophic veins present. Major secondary venation craspedodromous, secondary vein spacing increasing proximally, attachment to midvein excurrent.

Remarks. *Platanites* leaves commonly display palmate venation (i.e., actinodromous or palinactinodromous), with coarse teeth and lobes, and trifoliately compound leaves (McIver and Basinger, 1993; Manchester, 2014; Nares et al., 2025). The tooth morphology, venation pattern, and basal shape are consistent with the genus *Platanites*; although none of the specimens displays the compound leaflets typically diagnostic of the genus, the preserved morphological features are nonetheless sufficient to justify their assignment to *Platanites*, coupled with proximity to sites that also preserve *Platanites* leaves (Chandrasekharam, 1974; McIver and Basinger, 1993). Originally described from the middle Paleocene of Scotland (Forbes, 1851; Crane et al., 1988), the genus has also been documented in North America, where it is known from both Late Cretaceous (Maastrichtian) and Paleocene deposits from western Canada, the Canadian High Arctic, and the Rocky Mountain region of the United States (Bell, 1949; McIver and Basinger, 1993; Johnson, 1996; Manchester, 2014; West et al., 2019).

Order TROCHODENDRALES
Takht. ex Cronquist. 1981

Family TROCHODENDRACEAE
Eichler 1865

Genus *Nordenskioeldia* Heer 1870

Nordenskioeldia borealis Heer emend.
P.R Crane, Manchester et Dilcher 1991

Fig. 3H

Specimens examined. S10543.

Description. Fruits, ~11 mm in diameter, appear ovoid, globose, or subglobose; fruits are divided into smaller fruitlets, up to 11 fruitlets observed but many incomplete; fruitlets whorled around a central column.

Remarks. This specimen closely resembles fossil material previously identified as the species *Nordenskioeldia borealis* Heer (Crane et al., 1991). Crane et al. (1991) placed *Nordenskioeldia* within the Trochodendraceae; however, this taxonomic placement has been questioned and warrants further investigation (e.g. Doweld, 1998; Manchester et al., 2018). The frequent co-occurrence of *Zizyphoides flabella* leaves and *Nordenskioeldia* infructescences across a range of Paleocene fossil assemblages, including in the Highvale ACZ assemblage, provides evidence for a biological association between the two taxa (Crane et al., 1991). Fossil occurrences of *Nordenskioeldia* span a broad geographic range, having been reported from both mid- and high-latitude localities in North America, Spitsbergen, Greenland and East Asia (e.g. Heer, 1868, 1870; Hollick, 1936; Koch, 1963; Chandrasekharam, 1974; Crane et al., 1991; Kvaček et al., 1994; Budantsev and Golovneva, 2009; Moiseeva et al., 2018).

Genus *Zizyphoides*
Seward et V.M.Conway 1935
emend. Zolina, Manchester et Golovn. 2021

Zizyphoides flabella (Newb. 1863)
P.R.Crane, Manchester et Dilcher 1991

Fig. 3J

Specimens examined. S7721.

Description. Leaf nanophyllous to notophyllous, petiolate, attachment marginal, elliptic to ovate, length-to-width ratio about 1–1.5:1, medially symmetric, base symmetric; apex shape straight to acuminate, apex angle acute to obtuse; base shape truncate to concavo-convex, base angle obtuse. Leaf margin untoothed to weakly undulate. Primary venation actinodromous, with 3–5 basal veins. Major secondary venation brochidodromous.

Remarks. These leaves are easily identified to the well-documented Late Cretaceous and Paleocene species *Zizyphoides flabella* (Crane et al., 1991; Zolina et al., 2021). They are readily distinguished by their combination of morphological features, including long, slender petioles, palmate venation with conspicuous lateral primaries that strongly arch following near parallel course with the central primary vein, and ovate lamina with entire to undulate margins. The repeated association of *Zizyphoides flabella* leaves and *Nordenskioeldia* infructescences across a variety of Paleocene fossil assemblages, including the Highvale ACZ assemblage, suggests a biological connection between these two taxa (Crane et al., 1991). *Zizyphoides flabella* exhibits a broad palaeobiogeographic distribution across the Northern Hemisphere during the Late Cretaceous and Paleocene, with occurrences documented in western North America, Greenland, Spitsbergen and parts of north-eastern Asia (Crane et al., 1991; Zolina et al., 2021). The presence of *Zizyphoides* in both North America and Asia suggests that it may have dispersed across high-latitude land connections, such as the Bering land bridge, which facilitated floristic exchange between continents during the early Paleogene. Its consistent co-occurrence with *Nordenskioeldia* fruits across these regions supports the view that *Zizyphoides flabella* was part of a widespread and ecologically prominent plant lineage that played a significant role in Paleocene forest ecosystems (Crane et al., 1991; Zolina et al., 2021; Manchester, 2025).

Order SAXIFRAGALES
Bercht. et J. Presl. 1820

Family CERCIDIPHYLLACEAE Engl. 1907

Genus *Archeampelos* McIver
et Basinger 1993

Archeampelos lobocrenata
(Lesq. 1873) Doweld 2016

Fig. 3K

Specimens examined. S5472, S5483, S7719, S7741, S7796, S7798, S7802, S7814, S7819.

Description. Leaf microphyllous to mesophyllous, petiolate, attachment marginal, elliptic, length-to-width ratio about 1:1, medially symmetric, base symmetric; apex shape convex, apex angle acute; base shape truncate to weakly cordate, base angle obtuse to reflex. Leaf margin serrately crenate, with 2 orders of teeth, 1 tooth/cm, regular spacing, shape convex/convex, sinus rounded or angular, tooth apex glandular or retuse. Primary venation actinodromous, with 5–6 basal veins; simple agrophic veins present. Major secondary venation craspedodromous, sub-opposite or alternate, secondary vein spacing increasing proximally, secondary vein spacing regular, attachment to midvein excurrent.

Remarks. These fossils closely resemble specimens previously reported as *Archeampelos lobocrenata* from mid-latitude regions of North America, Alaska, Spitsbergen and

Russia (e.g. Newberry, 1868; Hollick, 1936; Bell, 1949; Brown, 1962; Chandrasekharam, 1974; McIver and Basinger, 1993; Budantsev and Golovneva, 2009; Peppe, 2009; Manchester, 2014; Moiseeva et al., 2018). This genus was initially assigned to the Vitaceae (Brown, 1962; McIver and Basinger, 1993), but Peppe (2009) challenged this placement, citing key foliar features, such as venation patterns and distinctive tooth morphology, as inconsistent with Vitaceae and more indicative of Cercidiphyllaceae. Manchester (2014) supported this reassignment in his revision of Brown's (1962) flora, noting that both the leaf architecture and the presence of marginal glands align more closely with characteristics of the Cercidiphyllaceae.

Genus *Trochodendroides*
E.W.Berry 1922

Trochodendroides genesevianum
(Chandrasekharam 1974) C.K.West,
Reichgelt et G.L.Hoffman comb. nov.

Fig. 4A

1974 *Cercidiphyllum genesevianum* Chandrasekharam; Palaeontographica Abt. B. (pl. 7, figs 51–60; pl. 8, figs 61–66, 68; pl. 9, figs 69–71; pl. 10, figs 74–77; pl. 11, figs 80–83; pl. 12, figs 84, 85).

Specimens examined. S7772.

Description. Leaf microphyllous, petiolate, attachment marginal, ovate, length-to-width ratio about 2:1, medially symmetric, base symmetric; apex shape acuminate, apex angle acute; base shape truncate, base angle obtuse. Leaf margin serrately crenate, with 1 order of teeth, 2–4 teeth/cm, regularly spaced, shape convex/convex to convex/concave; sinus rounded, apex glandular. Primary venation actinodromous, with 5 basal veins; simple agrophic veins present. Major secondary venation semicraspedodromous; secondary vein spacing regular; attachment to midvein excurrent.

Remarks. The specimen's features correspond closely with the concept of this fossil species, including its length-to-width ratio, acuminate apex, rounded base, and finely serrate-crenate margin bearing apical glands. Leaves of this type are distinguished from other *Trochodendroides* species by their more consistently elliptic outline, whereas related species tend to be broadly ovate to reniform. The combination of an acuminate apex and serrate margin further separates this species from other members of *Trochodendroides* within the Highvale flora. Another notable feature of this species is the presence of lateral primary veins that run largely parallel to the midvein, gently curving toward the apical portion of the lamina. The apex of the figured specimen (Fig. 4A) is acuminate but appears straight due to the loss of the leaf's fine apical tip, which has flaked away. Chandrasekharam's (1974) analysis of the extant genus *Cercidiphyllum* was thorough and highlighted notable overlap in foliar characteristics between the living taxon and fossil leaves from the Genesee locality. However, his classification of the fossil material was based solely on leaf morphology, without accompanying reproductive structures that would enable a definitive assignment to the modern genus. In the absence of such diagnostic evidence, we recommend reassigning these fossils to the form genus *Trochodendroides*, which is commonly used for leaves of this general morphology. Fossil fruits resembling those of *Cercidiphyllum* were recovered from the Genesee site, but these were not found in organic connection with any leaf material and were instead merely associated within the same assemblage. Notably, *Trochodendroides* is typically associated with the family Cercidiphyllaceae (Golovneva and Alekseev, 2017; Golovneva and Zolina, 2018), and thus the familial affinity suggested by Chandrasekharam is not disregarded by this more conservative taxonomic placement. Leaves attributed to *Trochodendroides* are common components of both Late Cretaceous and early Paleogene deposits across North America, Asia, and the High Arctic (Chandrasekharam, 1974; McIver and Basinger, 1993; Golovneva and Zolina, 2018; West et al., 2019; Manchester et al., 2023).

Trochodendroides flexuosa (Hollick 1936)
C.K.West, Reichgelt et G.L.Hoffman
comb. nov.

Fig. 4B

1936 *Populus flexuosa* Hollick; U.S. Geol. Surv. Prof. Paper 182, p. 63, pl. 33, fig. 2. [Basionym].

1974 *Cercidiphyllum flexuosa* (Hollick) Chandrasekharam; Palaeontographica Abt. B. (pl. 12, figs 86–88; pl. 13, figs 89, 90, 92–95).

Specimens examined. S7742, S7791.

Description. Leaf microphyllous to notophyllous, petiolate, attachment marginal,

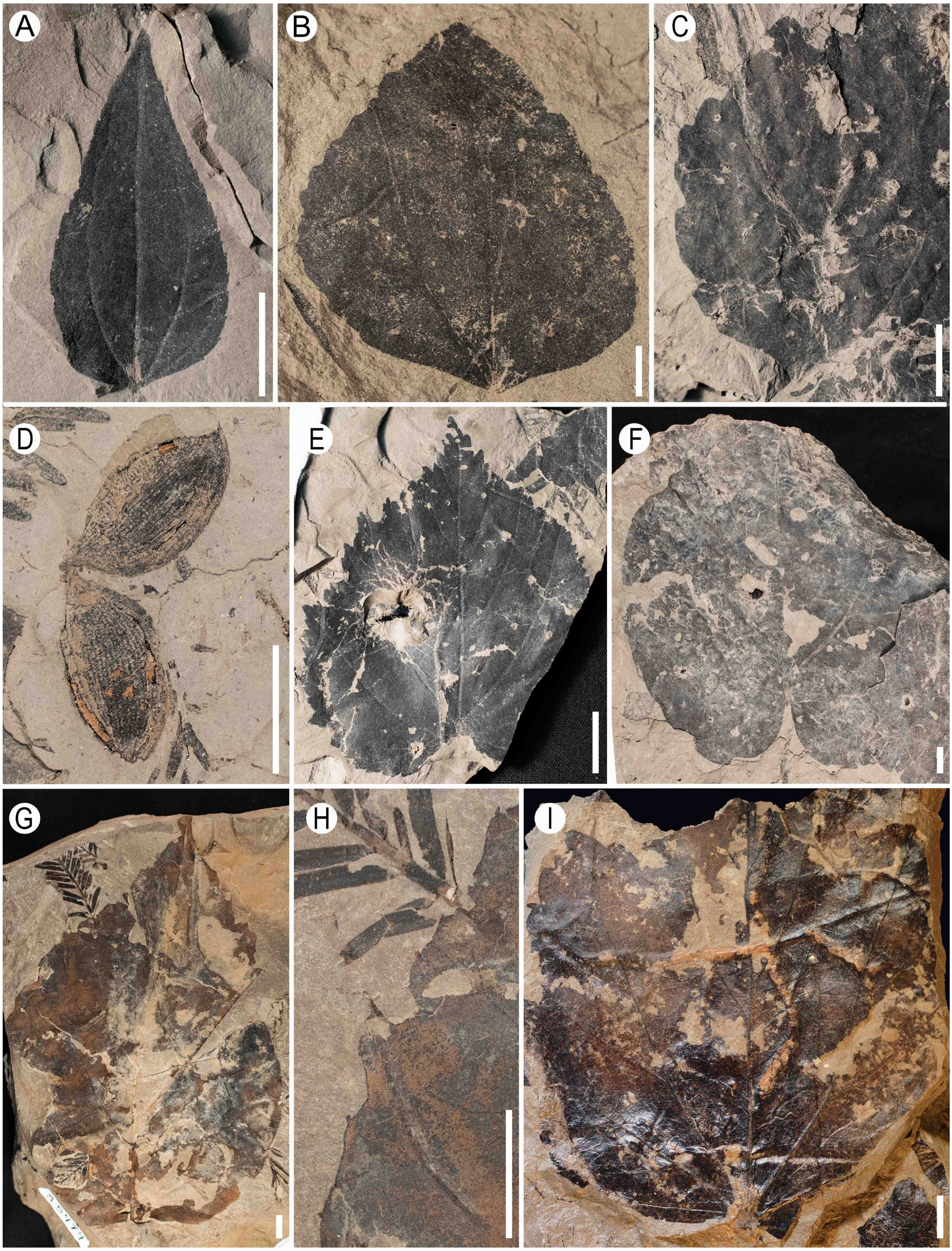

Figure 4. Fossils of the Highvale ACZ flora. **A**. *Trochodendroides genesevianum* comb. nov., leaf, S7772; **B**. *Trochodendroides flexuosa* comb. nov., leaf, S7742; **C**. *Trochodendroides cuneatum* comb. nov., leaf, S6853; **D**. *Jenkinsella arctica*, fruit, S5484; **E**. cf. *Craspedodromophyllum malmgrenii*, leaf, S7768; **F**. *Paranymphaea crassifolia*, leaf, S7721; **G**. cf. *Pterospermites* sp., leaf, S5474; **H**. Close up of teeth along the margin of specimen S5474; **I**. Unidentified leaf 6, S10542. Scale bars = 1 cm

ovate, length-to-width ratio about 1–1.5:1, medially symmetric, base symmetric; apex shape straight, apex angle obtuse; base shape truncate to concavo-convex, base angle obtuse. Leaf margin serrately crenate, with 1 order of teeth, 2–3 teeth/cm, regularly spaced, shape convex/convex to convex/concave; sinus rounded, apex simple. Primary venation actinodromous, with 3–5 basal veins; simple agrophic veins present. Major secondary venation festooned semicraspedodromous; secondary vein spacing gradually increasing proximally; attachment to midvein excurrent.

Remarks. These leaves correspond to material figured by Chandrasekharam (1974) and are characterized by an ovate lamina, a concavo-convex base, and festooned semicraspedodromous secondary venation. This species is primarily distinguished from other *Trochodendroides* species in the Highvale flora by its marginal morphology. The teeth are shallow to weakly crenate, with simple apices, and evenly spaced. In contrast, *T. genesevianum* possesses sharply serrate teeth, whereas *T. cuneatum* exhibits more coarsely crenate margins. Marginal characters provide reliable diagnostic value within the genus, as variation in tooth shape, size, density, and spacing has previously been used to differentiate *Trochodendroides* species (West et al., 2019).

Trochodendroides cuneatum
(Newb. 1898) C.K.West, Reichgelt
et G.L.Hoffman
comb. nov.

Fig. 4C

1898 *Populus cuneata* Newb.; U.S. Geol. Surv. Mon. 35, p. 41 [Basionym].

1974 *Cercidiphyllum cuneatum* (Newb.) Chandrasekharam; Palaeontographica Abt. B. (pl. 14, figs 97, 98, 101; pl. 15, figs 102, 104–108; pl. 16, figs 110, 111, 113–115; pls 17–19)

Specimens examined. S6853.

Description. Leaf microphyllous, petiolate, attachment marginal, elliptic, length-to-width ratio about 2:1, medially symmetric, base symmetric; apex shape straight, apex angle acute; base shape concavo-convex, base angle obtuse. Leaf margin coarsely crenate, with 1 order of teeth, 1–3 teeth/cm, irregularly spaced, shape convex/convex to convex/concave; sinus rounded, apex simple. Primary venation actinodromous, with 3 basal veins. Major secondary venation semicraspedodromous.

Remarks. Although represented by a single specimen, this leaf corresponds to material figured by Chandrasekharam (1974) and is characterized by an elliptic lamina, coarsely crenate margin, and an acute apex. Within the Highvale flora, *T. cuneatum* is readily distinguished from the other *Trochodendroides* species by its coarsely crenate teeth, which are irregularly spaced along the margin. This contrasts with the evenly spaced, shallowly crenate teeth of *T. flexuosa* and the sharply serrate teeth of *T. genesevianum*.

Genus *Jenkinsella*
E.Reid et M.Chandler 1933

Jenkinsella arctica
(Heer 1870) W.A.Bell 1949

Fig. 4D

Specimens examined. S5482, S5484, S7815.

Description. Dispersed fruits, elliptic to ovate, appear flattened, 15–19 mm long, 9–10 mm wide; apex rounded or acute, a possible persistent style present at the apex; base rounded or acute. Fruits with up to 14 parallel external longitudinal ridges.

Remarks. The dispersed fruits recovered from the Highvale ACZ are assignable to *Jenkinsella arctica* based on several key morphological features. These include an elliptic to ovate outline, rounded to acute apices and bases, and the presence of parallel longitudinal ridges on the fruit surface. This combination of characters is consistent with the species concept of *J. arctica* (Golovneva and Alekseev, 2017). *J. arctica* is a widespread component of Paleogene floras across the Northern Hemisphere and is frequently recovered from deposits in association with leaves of *Trochodendroides* (Golovneva and Alekseev, 2017), as is the case in the Highvale ACZ.

Order FAGALES Engl. 1892

Family BETULACEAE Gray 1822

Genus *Craspedodromophyllum*
P.R.Crane 1981

Craspedodromophyllum cf. ***C. malmgrenii***
(Heer 1868) Golovn. 2002

Fig. 4E

Specimens examined. S6854, S7737, S7755, S7768.

Description. Leaf microphyllous to mesophyllous, petiolate, attachment marginal, ovate, length-to-width ratio about 1–2:1, medially symmetric, base symmetric; apex angle acute, apex shape straight; base angle obtuse to reflexed, base shape cordate. Leaf margin serrate, with 2 orders of teeth, 4–6 teeth/cm, regularly spaced, shape straight/concave to convex/straight to convex/convex, sinus rounded, apex simple. Primary venation pinnate or pinnate-palmate, with 1 or 3 basal veins; compound agrophic veins present. Major secondary venation craspedodromous; secondary vein spacing irregular or gradually increasing proximally; secondary vein angle uniform; attachment to midvein excurrent. Tertiary venation opposite percurrent; tertiary vein angle obtuse to midvein; tertiary vein course straight to convex.

Remarks. This leaf resembles fossil foliage from Spitsbergen and from Ellesmere Island in Canada, referred to as *Craspedodromophyllum malmgrenii* (Golovneva, 2002; Budantsev and Golovneva, 2009; West et al., 2019). The pinnate to palmate-pinnate primary venation, craspedodromous secondary venation, doubly serrate margin with larger secondary teeth that can appear almost as small lobes, are all characteristics that align with this fossil species. *Craspedodromophyllum* was a fossil genus established by Crane (1981) to encompass leaf material found in close association with, though not physically attached to, the fossil fruit *Palaeocarpinus* Crane. *Craspedodromophyllum malmgrenii* differs from Crane's (1981) original concept of the genus, which emphasized only pinnate primary venation, whereas *C. malmgrenii* exhibits pinnate to palmate-pinnate venation. Budantsev and Golovneva (2009) based their assignment on the association of *C. malmgrenii* leaves with *Palaeocarpinus* fruits. However, the occurrence of palmate-pinnate venation in *C. malmgrenii* indicates that its placement within *Craspedodromophyllum* may warrant further consideration. Although *Palaeocarpinus* fruits have not been identified in the Highvale ACZ flora, the overall leaf architecture agrees with fossils previously described as *C. malmgrenii*. As the typically diagnostic fruits are absent, we regard the material as comparable to *C. malmgrenii* only and refrain from a firm assignment to this species. Fossil leaves resembling, or attributed to, *Craspedodromophyllum* have been documented across a range of early Paleogene sites, including localities in North America, Spitsbergen, Scotland and Russia (e.g. Crane, 1981, and references therein; Boulter and Kvaček, 1989; Sun and Stockey, 1992; Golovneva, 2002; Budantsev and Golovneva, 2009; Moiseeva et al., 2018; West et al., 2019).

Order CARYOPHYLLALES
Juss. ex Bercht. et J. Presl. 1820

Family POLYGONACEAE Juss. 1789

Genus *Paranymphaea* E.W.Berry 1935

Paranymphaea crassifolia
(Newb. 1868) E.W.Berry 1935
Fig. 4F

Specimens examined. S7721, S7763.

Description. Leaf microphyllous to mesophyllous, petiolate, attachment marginal, ovate, medially symmetric, base symmetric; base angle reflexed, base shape cordate. Leaf margin untoothed. Primary venation basal actinodromous, with 3 or 5 primary veins, primary vein thickness 1.21 mm, lateral primary vein thickness 1.01–1.05 mm; simple agrophic veins present. Major secondary venation brochidodromous; secondary vein spacing gradually increasing proximally; secondary vein angle uniform; attachment to midvein excurrent.

Remarks. These specimens closely resemble material from other early Paleocene localities in Canada that have been referred to the species *Paranymphaea crassifolia* (McIver and Basinger, 1993). The leaf fossil taxon *Paranymphaea crassifolia*, originally thought to resemble aquatic plants like *Nymphaea*, was re-evaluated in detail by McIver and Basinger (1993) and found to differ significantly from the Nymphaeaceae in both morphology and ecology. Although its overall venation superficially resembles that of some *Nymphaea* species, close inspection revealed several key distinctions: differences in leaf shape, petiole position, the absence of aerenchyma, and distinct venation architecture, including the presence of intersecondary veins and a marginal vein. These features, along with the leaf's chartaceous texture and lack of consistent association with other aquatic taxa, argue against a hydrophytic lifestyle and exclude *Paranymphaea* from the Nymphaeaceae (McIver and Basinger, 1993). Instead, the fossil displays a suite of characteristics more consistent with the Polygonaceae (McIver and Basinger, 1993). As opposed to an aquatic or semi-aquatic habit, the inferred growth habit of *Paranymphaea* is instead a basal herbaceous rosette or a low-lying shrub (McIver and Basinger, 1993).

Order CORNALES Link 1829

Family NYSSACEAE Juss. ex Dumort. 1829

Genus *Browniea*
Manchester et L.Hickey 2007

Browniea serrata
(Newb. 1868) Manchester et L.Hickey 2007
Fig. 5A

Specimens examined. S5455, S5458, S5476, S7718, S7811.

Description. Leaf notophyllous to mesophyllous, petiolate, attachment marginal, elliptic, length-to-width ratio about 1.5–2:1, medially symmetric, base symmetric; apex shape straight, apex angle obtuse to acute. Leaf margin serrately crenate, with 1 order of teeth, 1–6 teeth/cm, regularly spaced, shape straight/convex, convex/convex, convex/concave, straight/concave; sinus angular, apex simple. Primary venation pinnate, with 1 basal vein; agrophic veins absent. Major secondary venation craspedodromous or semicraspedodromous; secondary vein spacing regular; secondary vein angle uniform; attachment to midvein excurrent.

Remarks. *Browniea* is an extinct genus of Nyssaceae described by Manchester and Hickey (2007) based on abundant fossil material, including both foliage and reproductive material, from the Paleocene of North America. The type species, *Browniea serrata*, had a long history of taxonomic misassignment prior to its formal recognition. Leaves of this species were previously attributed to a range of unrelated genera, including *Alnus*, *Celastrus*, *Eucommia*, and *Tapiscia* due to their simple form and serrated margins (Manchester and Hickey, 2007). Fossil remains of *Browniea* have been recovered from numerous sites across the western interior of North America, including Wyoming, Montana, North and South Dakota, Colorado, Alberta, and Saskatchewan (Manchester and Hickey, 2007; Manchester, 2014). These range from the latest Cretaceous (Maastrichtian) into the late Paleocene (upper Clarkforkian), indicating that *Browniea* was a persistent and ecologically successful component of mid-latitude Paleocene forests (Manchester and Hickey, 2007). The widespread distribution of *Browniea serrata* and frequent co-occurrence with other nyssaceous taxa, such as *Amersinia* and *Davidia*, underscore the ecological importance and taxonomic diversity of the Nyssaceae during the early Paleogene in North America (Manchester and Hickey, 2007).

Family Incertae Sedis

Genus cf. *Pterospermites* Heer 1859

cf. ***Pterospermites*** sp.
Fig. 4G, H

Specimens examined. S5473, S5474, S7789.

Description. Leaf mesophyllous, petiolate, attachment marginal, ovate to elliptic, length-to-width ratio about 1.5:1, medially symmetric, base symmetric; apex shape straight, apex angle acute; base shape truncate to cordate, base angle obtuse to reflexed. Leaf margin serrate, with 1 order of teeth, 2 teeth/cm, teeth small, peg or hook-like, shape retroflexed/convex or convex/retroflexed, regularly spaced, sinuses rounded. Primary venation pinnate, with 1 basal vein; simple agrophic veins present. Major secondary venation craspedodromous; secondary vein spacing decreasing proximally; attachment to midvein excurrent. Tertiary venation opposite percurrent; tertiary vein angle obtuse to midvein; tertiary vein course straight.

Remarks. This specimen closely resembles *Pterospermites dawsonii* (Knowlt.) W.A.Bell in overall lamina shape, as well as in the form of the apex, base, and general size. However, the Highvale specimen differs markedly in marginal morphology. Its teeth are small, weakly crenate, and bear peg- or hook-like projections at the apices. In contrast, the teeth of *P. dawsonii*, when present, are much larger, sharply serrate, and often irregularly spaced along the margin (Bell, 1949). In Canadian floras, *Pterospermites dawsonii* is known primarily from Paleocene assemblages, including those of Alberta and Saskatchewan, where it is a moderately frequent component of fluvial and deltaic deposits (Bell, 1949). It is characterized by ovate, elliptic, or obovate leaves with toothed or entire margins, and a prominent petiole

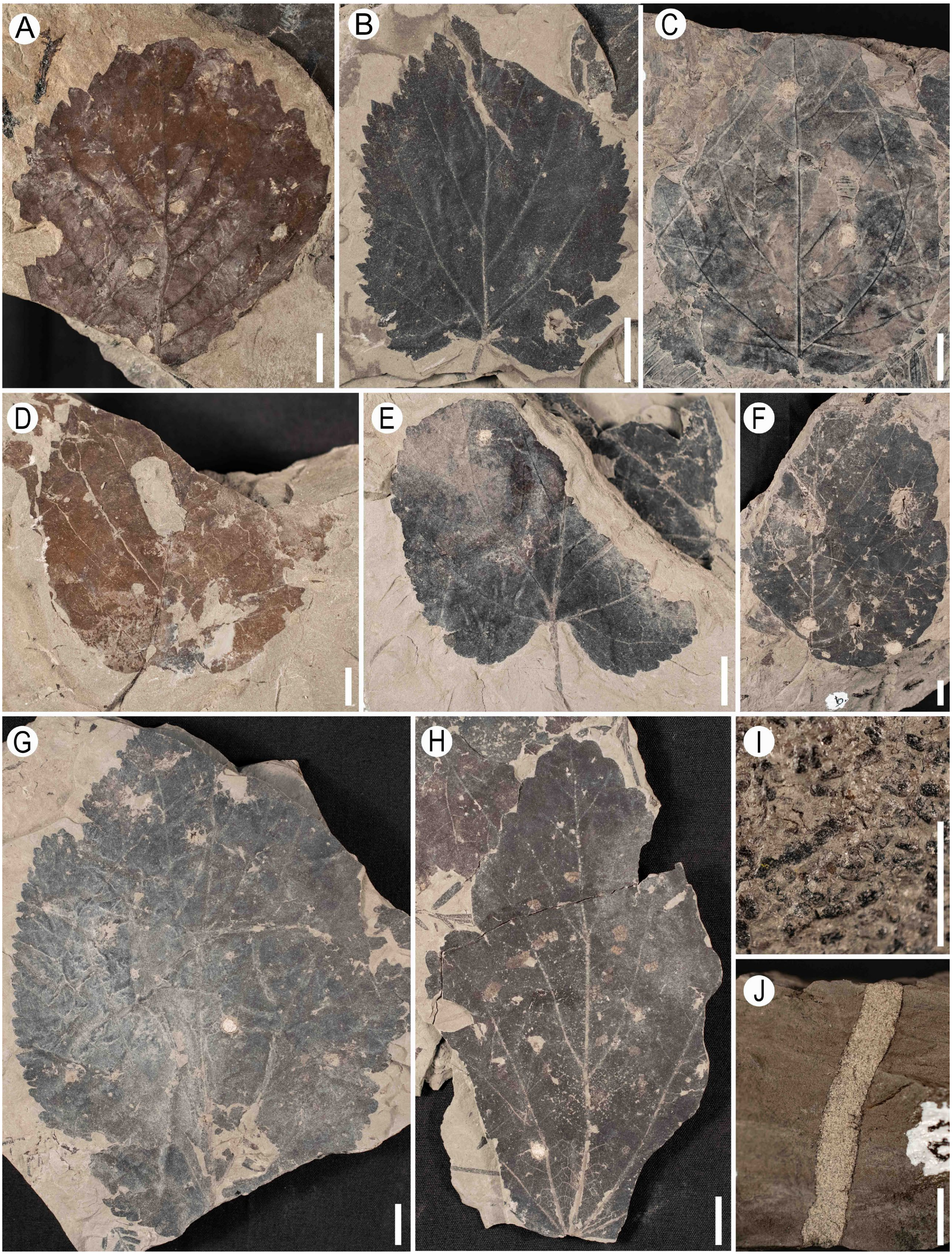

Figure 5. Fossils of the Highvale ACZ flora. **A**. *Browniea serrata*, leaf, S5476; **B**. Unidentified leaf 1, S7812; **C**. Unidentified leaf 2, S7754; **D**. Unidentified leaf 8, S7745; **E**. Unidentifed leaf 5, S5461; **F**. Unidentified leaf 4, S6878; **G**. Unidentified leaf 7, S7807; **H**. Unidentified leaf 3, S7816; **I**. Unidentified seeds, S7733; **J**. Unidentified stem casts, S7775. Scale bars = 1 cm

(Bell, 1949). The genus *Pterospermites* was originally established for winged seeds from the Miocene (see Manchester, 2014), and its use for leaves has been discouraged (Wolfe, 1966; Hickey, 1977). Hickey (1977) erected the new genus *Penosphyllum* to accommodate leaves originally assigned to *Pterospermites*; however, the morphological characters attributed to *Pterospermites* are much broader than those described for *Penosphyllum*. As such, the fossils from the Highvale ACZ do not conform to the concept of *Penosphyllum*. Nevertheless, the marginal morphology of the Highvale specimens also differs from that typical of *Pterospermites dawsonii*. The name *Pterospermites dawsonii* is referenced here to maintain continuity with its established use in other early Paleocene floristic assemblages from Canada (see Bell, 1949), although the Highvale material is compared only at the generic level. The systematic affinities of *P. dawsonii* remain uncertain, as the species exhibits considerable morphological variability and may not represent a natural taxon.

Unidentified leaf 1

Fig. 5B

Specimen examined. S7812B.

Description. Leaf microphyllous, petiolate, attachment marginal, elliptic, length-to-width ratio about 1.2:1, medially symmetric, base symmetric; base shape cordate, base angle reflexed. Leaf margin serrate, with 2 orders of teeth, 6 teeth/cm, shape convex/convex, regularly spaced, sinuses angular. Primary venation basal actinodromous, with 3 basal veins; compound agrophic veins present. Major secondary venation craspedodromous; secondary vein spacing irregular; attachment to midvein excurrent. Tertiary venation opposite percurrent; tertiary vein angle obtuse to midvein; tertiary vein course straight.

Remarks. This leaf is represented by a single, isolated specimen and cannot be confidently assigned to any known taxon, although it bears some resemblance to leaves previously referred to *Vitis*. However, given that it is represented by a single specimen, we do not follow this assignment at this time. The leaf is characterized by its elliptic shape with a cordate base and displays actinodromous primary venation with three basal veins. The margin is distinctly serrate, bearing regularly spaced compound teeth. This leaf bears superficial resemblance to the specimen referred to cf. *Craspedodromophyllum malmgrenii* but differs in several key respects. Most notably, it possesses compound agrophic veins, whereas cf. *C. malmgrenii* exhibits only simple agrophic veins. The marginal teeth are also distinct, being more rounded with a convex–convex profile, in contrast to the straight–concave to convex–straight, and only rarely convex–convex, teeth of cf. *C. malmgrenii*. In addition, this specimen has an elliptic lamina, whereas leaves of cf. *C. malmgrenii* are typically ovate.

Unidentified leaf 2

Fig. 5C

Specimen examined. S7754.

Description. Leaf notophyllous, petiolate, attachment marginal, ovate, medially symmetric, base symmetric; base shape rounded, base angle obtuse. Leaf margin serrately crenate or crenulate, with 1 order of teeth, 1 tooth/cm, shape convex/convex, irregularly spaced, sinuses rounded. Primary venation palinactinodromous, with 3 basal veins, primary vein thickness 0.80 mm, lateral primary vein thickness 0.58–0.61; simple agrophic veins present. Major secondary venation craspedodromous; secondary vein spacing irregular; attachment to midvein excurrent; intersecondary veins present.

Remarks. This leaf is known from a single specimen and does not correspond to any previously described taxon. As such, it remains unidentified. The leaf is characterized by a serrate margin with irregularly spaced crenate teeth and a palinactinodromous venation pattern, but the absence of diagnostic features or comparable material precludes confident taxonomic assignment at this time.

Unidentified leaf 3

Fig. 5G

Specimen examined. S7816.

Description. Leaf notophyllous, attachment marginal; apex shape straight, apex angle obtuse. Leaf margin serrately crenate, with 1 order of teeth, 2 teeth/cm, shape convex/convex, regularly spaced, sinuses rounded. Primary venation basal actinodromous, with 6 basal veins. Major secondary venation craspedodromous; secondary vein spacing decreasing proximally; attachment to midvein excurrent; interior secondary veins present. Tertiary venation opposite percurrent; tertiary vein angle obtuse to midvein; tertiary vein course convex.

Remarks. This leaf is distinguished by its actinodromous primary venation, with six basal veins radiating from the base, and a crenate margin. Although its overall morphology is distinctive, the specimen lacks sufficient diagnostic features for confident taxonomic placement and remains unidentified.

Unidentified leaf 4

Fig. 5H

Specimen examined. S6878.

Description. Leaf mesophyllous, petiolate, attachment marginal; base angle obtuse. Leaf margin appears untoothed with possible rare teeth in the apical portion. Primary venation pinnate, with 1 basal vein. Major secondary venation appears semicraspedodromous or brochidodromous.

Remarks. This leaf is represented by a single, fragmentary specimen. It exhibits apparent semicraspedodromous or brochidodromous secondary venation, basal asymmetry, and an untoothed margin with some possible teeth in the apical portion of the lamina, although both the basal asymmetry and the apparent teeth in the apical portion may be the result of margin damage. Due to its incomplete preservation and limited diagnostic features, the specimen remains unidentified.

Unidentified leaf 5

Fig. 5E

Specimen examined. S5461.

Description. Leaf mesophyllous, petiolate, attachment marginal; base shape cordate, base angle reflexed. Leaf margin crenately dentate, with 1 order of teeth, 3–4 teeth/cm, shape convex/convex, regularly spaced, sinuses rounded. Primary venation basal actinodromous, with 3 basal veins; simple agrophic veins present. Major secondary venation craspedodromous, attachment to midvein decurrent. Tertiary venation alternate percurrent; tertiary vein angle obtuse to midvein.

Remarks. This leaf is characterized by a broadly cordate base, crenately dentate margin, and actinodromous primary venation with three basal veins. Although the combination of these features is distinctive, the specimen lacks additional diagnostic traits necessary for precise taxonomic assignment and remains unidentified.

Unidentified leaf 6

Fig. 4I

Specimen examined. S10542.

Description. Leaf mesophyllous, attachment marginal, appears weakly lobed, base angle obtuse. Leaf margin toothed on lobes in the upper 1/3 of the leaf lamina and untoothed in the lower 1/3 to 2/3 of the lamina. Leaf teeth on lobes crenately serrate, with 1 order of teeth, shape convex/convex. Primary venation basal actinodromous, with 6 basal veins; agrophic veins appear absent. Major spacing of secondary veins irregular, attachment to midvein excurrent. Minor secondary vein course appears brochidodromous.

Remarks. Represented by a single specimen, this leaf is fragmentary but appears to be weakly lobed. Because the apical portion is missing, the depth of incision toward the midvein cannot be measured precisely, making it uncertain whether the projections represent true lobes or large marginal teeth. One probable lobe bears two prominent teeth on its apical and basal flanks, whereas the opposing lobe appears untoothed. The basal portion of the lamina lacks teeth, and although preservation is incomplete, the margin seems to remain entire along the lower one-third to two-thirds of the leaf. Given the limited number of diagnostic features and the fragmentary condition of the specimen, confident taxonomic assignment is not possible.

Unidentified leaf 7

Fig. 5F

Specimens examined. S7773, S7807.

Description. Leaf mesophyllous, petiolate, attachment marginal, base shape concave or cuneate, base angle acute. Leaf margin serrately crenate, with 1 order of teeth, 3 teeth/cm, shape convex/convex, regularly spaced, sinuses rounded. Primary venation appears basal actinodromous or possibly pinnate. Major secondary venation craspedodromous.

Remarks. This leaf is characterized by its robust serrate-crenate margin with multiple closely packed teeth, large size, long petiole, and tightly angled secondary venation. Although its morphology is distinctive, the limited amount of material and diagnostic features preclude an identification at this time.

Unidentified leaf 8

Fig. 5D

Specimen examined. S7745.

Description. Leaf notophyllous, petiolate, attachment marginal; base shape truncate, base angle obtuse. Leaf margin serrate, with 1 order of teeth, 2–3 teeth/cm, shape straight/convex or concave/convex, regularly spaced, sinuses rounded. Primary venation pinnate, with 1 basal vein. Major secondary venation craspedodromous.

Remarks. This leaf fragment bears distinctive, prominently serrate teeth, each defined by a short, curved distal flank, a long, straight proximal flank, and rounded sinuses. No other leaves from the Highvale ACZ assemblage exhibit teeth of this morphology. However, as the specimen is both fragmentary and singular, taxonomic identification is not possible at this time.

Unidentified seeds

Fig. 5I

Specimen examined. S7729A–D.

Description. Seeds dispersed, shape elliptic, ovate, or obovate, 2–2.5 mm long, about 1 mm wide; apex rounded, base rounded.

Remarks. These small seeds were found in a dense cluster (up to more than 20 seeds per cm^2) on one specimen, but they lack diagnostic features that could indicate their affinity.

Unidentified roots

Fig. 3L

Specimen examined. S7731.

Description. Roots, about 40 mm long; with rootlets, up to 7.5 mm long, branching from the main axis at right angles.

Remarks. Fossil roots like the example in Fig. 3L provide evidence of the recycling of organic matter by the Highvale ACZ plant community, but they lack diagnostic features that would allow the identification of their parent plants.

Unidentified stem casts

Fig. 5J

Specimens examined. S6878, S7768, S7775, S7813, S7820, S7754, S7807, S7816.

Description. Casts of plant stems, vertical, 2–7 mm in diameter, more than 3.5 cm long, cylindrical, circular to ovoid in cross-section, with a smooth carbonaceous margin about 0.1 mm thick; interior not preserved, filled with light-coloured, very fine-grained sand.

Remarks. These sand-filled stem casts are present in many of the Highvale ACZ specimens (e.g. Fig. 5E–H), in a few cases at densities of up to 3 or 4 stems per 10 cm^2 (i.e. S7813). They are identified as plant remains, rather than animal burrows, by their thin carbonaceous margins, but they cannot be identified further due to their lack of other morphological details.

PALAEOCLIMATE AND PALAEOENVIRONMENT

The ensemble palaeoclimate reconstruction method yielded broadly similar results for both the Highvale ACZ and Genesee floras, placing each within the temperate seasonal forest category of Whittaker's (1962, 1975) biome classification system (Fig. 6). For the Highvale ACZ fossil flora, the reconstructed mean annual temperature (MAT) is 9.6 ± 4.5°C, warmest quarter temperature (WQT) is 18.8 ± 4.3°C coldest

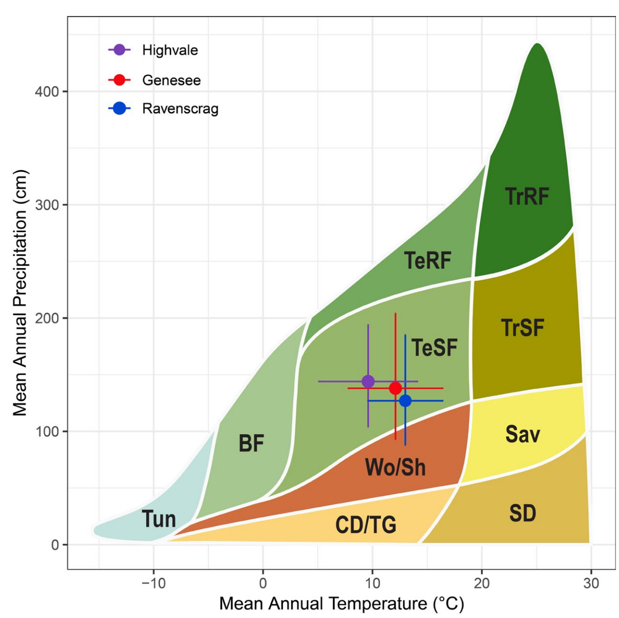

Figure 6. Whittaker Biome plot of the Highvale, Genesee, and Ravenscrag fossil floras. Tun = Tundra, BF = Boreal Forest, TeRF = Temperate Rainforest, TeSF = Temperate Seasonal Forest, Wo/Sh = Woodland/Shrubland, CD/TG = Cold Desert or Temperate Grassland, TrRF = Tropical Rainforest, TrSF = Tropical Seasonal Forest, Sav = Savanna, SD = Subtropical Desert

Table 2. Palaeoclimate estimates for the Highvale ACZ fossil flora. NLR = Nearest Living Relative, LAA = Leaf Area Analysis, LMA = Leaf Margin Analysis, MAT = Mean Annual Temperature, WQT = Warmest Quarter Temperature, CQT = Coldest Quarter Temperature, MAP = Mean Annual Precipitation, WMP = Warmest Month Precipitation, DMP = Driest Month Precipitation, RH = Relative Humidity, NPP = Net Primary Productivity

	Ensemble	CLAMP	NLR	LAA	LMA
MAT (°C)	9.6 ± 4.5	7.2 ± 2.1	15.8 (13.0–17.8)	–	6.5 ± 2.7
WQT (°C)	18.8 ± 4.3	15.1 ± 2.6	22.7 (20.2–24.9	–	–
CQT (°C)	2.7 ± 4.5	−1.1 ± 3.2	6.3 (3.3–9.3)	–	–
MAP (cm/yr)	144 +55/−40	140 +68/−46	132 (107–170)	167 +72/−50	–
WMP (cm)	–	19.1 + 11.1/−7.0	–	–	–
DMP (cm)	4.0 +7.6/−2.1	4.2 +5.4/−2.3	3.5 (2.1–6.2)	–	–
RH (%)	–	76.8 ± 9.2	–	–	–
NPP (gC m^{-2} yr^{-1})	–	701 +354/−282	–	–	–

quarter temperature (CQT) is 2.7 ± 4.5°C, mean annual precipitation (MAP) is 144 +55/−40 cm/yr, and the driest month precipitation (DMP) is 4.0 +7.6/−2.1 cm. Relative humidity (RH), estimated from CLAMP, is 76.8 ± 9.2%, with a net primary productivity (NPP) of 701 +354/−282 gC m^{-2} yr^{-1} (Table 2). The Genesee flora shows comparable values, with MAT = 12.1 ± 4.3°C, WQT = 19.5 ± 4.1°C, CQT = 4.0 ± 4.7°C, MAP = 138 +66/−45 cm/yr, and DMP = 3.5+3.1/−1.6 cm. CLAMP estimates an RH of 87.1 ± 9.2% and an NPP of 545 +317/−245 gC m^{-2} yr^{-1} (Table 3). In general, the precipitation estimates across proxy methods are consistent (Tables 2, 3); however, temperature estimates diverge between proxies, with the leaf physiognomic proxies producing cooler results than the NLR analysis (Tables 2, 3). The divergent outcomes of these proxies highlight the strength of the ensemble approach, which integrates reconstructions and their uncertainties to produce a more holistic palaeoclimate reconstruction without weighting one method over another. The palaeoclimate results suggest both sites supported broadly similar forested environments under relatively humid and seasonally temperate conditions.

Results from the closest climatic analogue analysis show that Highvale and Genesee had the strongest climatic similarities to regions in China, the Mediterranean and the Pacific Northwest (PNW) (Fig. 7). In China, both Highvale and Genesee are most closely aligned with Cfa climates (temperate, no dry season, hot summer), with a secondary resemblance to Cwa climates (temperate, dry winter, hot summer). In the Mediterranean region, Highvale was most similar to Cfb climates (temperate, no dry season, warm summer), with additional but less similarity to Cfa and limited resemblance to Csb climates (temperate, dry summer, hot summer). In contrast, Genesee aligned most strongly with Csa climates (temperate, dry summer, warm summer), though it also showed some similarity to Cfb and Cfa climates. In the PNW, Highvale showed the greatest similarity to Cfb climates, followed by some resemblance to Dfb climates (cold, no dry season, warm summer) and limited similarity to Dsb climates (cold, dry summer, warm summer). Genesee, on the other hand,

Table 3. Palaeoclimate estimates for the Genesee fossil flora. LAA result from Greenwood and West (2017). NLR = Nearest Living Relative, LAA = Leaf Area Analysis, LMA = Leaf Margin Analysis, MAT = Mean Annual Temperature, WQT = Warmest Quarter Temperature, CQT = Coldest Quarter Temperature, MAP = Mean Annual Precipitation, WMP = Warmest Month Precipitation, DMP = Driest Month Precipitation, RH = Relative Humidity, NPP = Net Primary Productivity

	Ensemble	CLAMP	NLR	LAA
MAT (°C)	12.1 ± 4.3	8.3 ± 2.1	15.6 (14.3–17.9)	–
WQT (°C)	19.5 ± 4.1	15.9 ± 2.6	23.0 (21.2–25.0)	–
CQT (°C)	4.0 ± 4.7	0.1 ± 3.2	8.3 (5.5–10.4)	–
MAP (cm/yr)	138 + 66/−45	104 + 51/−34	132 (112–155)	186 + 80/−56
WMP (cm)	–	16 + 9.3/−5.8	–	–
DMP (cm)	3.5 + 3.1/−1.6	3.9 + 4.9/−2.1	3.5 (2.1–5.0)	–
RH (%)	–	87.1 ± 9.6	–	–
NPP (gC m^{-2} yr^{-1})	–	545 + 317/−245	–	–

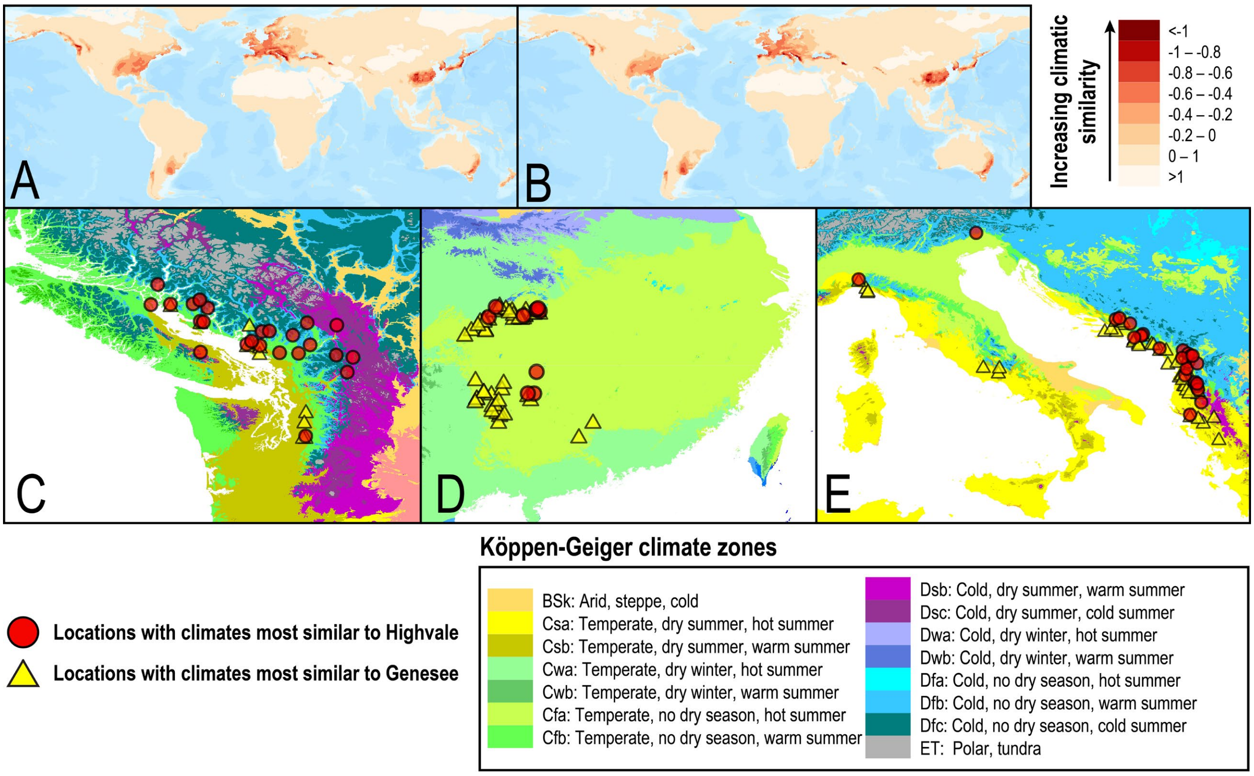

Figure 7. Graphical results of the closest climatic analogue analysis for (A) the reconstructed Highvale palaeoclimate and (B) the reconstructed Genesee palaeoclimate where dark reds indicate greater similarity and lighter pinks indicate greater dissimilarity. (C) Climatic similarity in the Pacific Northwest, (D) Climatic similarity in China, (E) Climatic similarity in the Mediterranean. Red circles represent locations with climates most similar to the reconstructed climate for the Highvale Mine region. Yellow triangles represent locations with climates most similar to the reconstructed climate for the Genesee region

most closely resembled Csb climates, with more limited similarity to Cfb climates in this region.

DISCUSSION

The Highvale ACZ fossil flora comprises a diverse assemblage of taxa, including *Metasequoia*, *Glyptostrobus*, *Equisetum*, *Osmunda*, *Trochodendroides*, *Browniea*, *Platanites*, *Paranymphaea*, *Zizyphoides* and multiple unidentified broadleaf 'dicots'. This combination of taxa suggests a temperate, mesic forest ecosystem with strong affinities to riparian or palustrine environments. The dominance of *Metasequoia* and *Glyptostrobus*, both typically deciduous conifers associated with swamp and floodplain habitats, implies persistent or seasonal waterlogging in a deltaic, palustrine, or floodplain setting (LePage et al., 2005; LePage, 2007; Averyanov et al., 2009). These genera are frequently documented in Paleogene assemblages representing humid climates with equable or seasonally variable conditions (Bell, 1949; Brown, 1962; Chandrasekharam, 1974; Hickey, 1977; McIver and Basinger, 1993; Manchester, 2014; Greenwood and West, 2017; West et al., 2019, 2021).

Many of the broadleaf taxa in the ACZ flora (e.g. *Trochodendroides*, *Platanites*, *Browniea* and *Zizyphoides*) are thought to have been deciduous, with modern relatives supporting this interpretation (Crane et al., 1991; McIver and Basinger, 1993; Manchester, 1999; Manchester and Hickey, 2007). Similar taxa in the Ravenscrag Butte flora were reconstructed as deciduous using a leaf mass per area proxy (see West et al., 2021), and the same likely applies to the Highvale ACZ fossil flora. In warm, higher latitude Paleogene forests, evergreen plants may have been disadvantaged by winter respiration losses under low-light conditions, compared to deciduous species that could enter dormancy triggered by photoperiod reduction (Parrish and Spicer, 1988; West et al., 2015, 2024). The abundance of deciduous taxa supports the idea that the Highvale region during the early Paleocene had a seasonal climate, potentially resulting from some combination of differences in light availability, temperature and water availability.

The microflora of the Highvale ACZ coals is consistent with this picture. Palynofloral analysis of coal samples indicates that peat accumulation occurred in freshwater swamps that ranged from forested wetlands with cupressaceous trees to open marshes with herbaceous plants (Demchuk and Hills, 1991; Demchuk, 1992). The assemblages appear to be dominated by the taxodioid palynomorph *Taxodiaceaepollenites hiatus* (Demchuk and Hills, 1991; Demchuk, 1992). Also present are spores of osmundaceous and polypodiaceous ferns; spores of *Sphagnum* L. and other mosses; and pinaceous pollen, some of which may have been brought into the wetlands by prevailing winds (Demchuk and Hills, 1991; Demchuk, 1992). Angiosperm pollen is minor and consists of ulmaceous and betulaceous species (Demchuk and Hills, 1991; Demchuk, 1992).

Sedimentological data from the Highvale section reinforce the interpretation of a low-energy, seasonally wet floodplain environment. Clastic input was minimal during the late stages of peat accumulation: clastic interbeds near the top of Seam 1 are few, thin and discontinuous (Demchuk, 1992; Demchuk et al., 1993). Peat accumulation was followed by an increase in low-energy fluvial activity that covered the organic soils of the peatlands with silty mud (Demchuk, 1992; Demchuk et al., 1993), likely acting to preserve the plant fossils described herein. The fine-grained, carbonaceous character of the mudstones and the presence of rooting structures suggest damp soils and episodic, low-energy flooding (Demchuk, 1992; Demchuk et al., 1993). These conditions would have been favourable for both plant growth and preservation.

Plants are best preserved under reducing, acidic conditions where microbial decomposition is suppressed (Retallack, 1997). Such environments typically occur in waterlogged soils, where the accumulation of organic acids reduces pH and oxidation–reduction potential. Many specimens from the Highvale ACZ fossil flora are fragmentary, but the large, nearly complete leaves of *Pterospermites* and *Paranymphaea* and rooted sedimentary horizons suggest that the assemblage is largely autochthonous. The limited fragmentation that is present may reflect relatively in situ burial and decomposition rather than long-distance transport. This suggests that waterlogged, reducing conditions may have been episodic, with periodic flooding events introducing fresh water, diluting the organic acids that lower the pH, and thus allowing for intervals of microbial decay. Ultimately, the reducing environments necessary for preserving terrestrial plant remains were likely maintained by persistent waterlogging between episodic flooding events.

The modern analogues of many ACZ taxa also support the interpretation of a humid, seasonally inundated forest mosaic. *Metasequoia glyptostroboides* grows in riparian and disturbed habitats with ample moisture (LePage et al., 2005), and *Glyptostrobus pensilis* occupies swampy lowlands (LePage 2007; Averyanov et al., 2009). *Equisetum* and *Osmunda* are typical of marshes and wet meadows (Miller Jr., 1967; Pearce and Cordes, 1988). *Browniea serrata*, possibly ecologically similar to extant *Nyssa*, likely tolerated periodic flooding and grew along stream and lake margins (Manchester and Hickey, 2007). *Paranymphaea* may indicate localized disturbance or fluctuating water levels within a spatially heterogeneous floodplain (McIver and Basinger, 1993).

Comparison with other western Canadian early Paleocene floras provides further ecological context. Dominant taxa such as *Browniea*, *Trochodendroides* and *Archeampelos* are shared with the nearby Genesee flora (Chandrasekharam, 1974; Manchester, 2014; Greenwood and West, 2017), although direct comparison is limited by the number of unidentified taxa. Overlap with the early Paleocene Ravenscrag Butte flora from southwestern Saskatchewan includes taxa, such as *Platanites*, *Paranymphaea* and *Trochodendroides* (McIver and Basinger, 1993). Curiously, the Genesee flora contains the only palm fossil, *Sabalites geneseensis* D.R.Greenwood et C.K.West (Greenwood and West, 2017), suggesting that the conditions of the Genesee area were more suitable for palms than those at either Highvale or Ravenscrag. The unique elements found at each site (e.g. *Craspedodromophyllum* at Highvale; *S. geneseensis* at Genesee; *Mciveraephyllum* (Schimper) Manchester and *Sapindus* L. at Ravenscrag) suggest real ecological differences rather than taphonomic artifacts. Similar depositional environments but differing floristic composition suggest some degree of regional and/or temporal heterogeneity in early Paleocene vegetation.

Palaeoclimate reconstructions of the Highvale and Genesee floras generally point toward temperate humid environments with a distinct dry season (Tables 2, 3). These early Paleocene climates are notably warmer and wetter than the climate in this area today; for example, the MAT of Edmonton and Calgary is between 4 and 4.5°C and MAP between 40 and 45 cm (Environment and Climate Change Canada, 2025). Both Edmonton and Calgary are classified as cold climates lacking a dry season and with a warm summer in the Köppen-Geiger scheme (Beck et al., 2018), although they are geographically and climatically close to the steppe climates farther east. By contrast, the early Paleocene regional environment would have been temperate, characterized by warm to hot summers and either a dry summer or no dry season, depending on which month was the driest (Beck et al., 2018). Genesee has a notably warmer reconstructed climate than Highvale (though within error), differing by approximately 2.5°C over less than one degree of latitude (Tables 2, 3), which may reflect a latitudinal gradient, but this degree of change may also be the result of microclimatic variation, depositional bias, or sampling uncertainty. In contrast, the early Paleocene Ravenscrag Butte flora from southern Saskatchewan, with a reconstructed MAT of 13.0 ± 3.4°C (West et al., 2021), lies approximately 4 degrees farther south of Genesee yet is only about 1°C warmer. This equates to a temperature gradient of roughly 0.25°C per degree of latitude. The trend of increasing temperature among sites with decreasing latitude is consistent with latitudinal climate gradients across western North America proposed for the Paleocene and Eocene (Greenwood and Wing, 1995; Zhang et al., 2019). Additionally, precipitation estimates between the three sites suggest increasing moisture availability with latitude as well (Tables 2, 3; West et al., 2021).

Although seasonally dry conditions were estimated for all sites (Tables 2, 3; West et al., 2021), overall moisture availability remained high, as reflected in relative humidity values across the sites (all >75%), which suggests all three sites were consistently moist environments. Palaeoclimate and palaeoenvironmental reconstructions indicated that the Ravenscrag Butte forest was a lush, seasonally dynamic, warm-temperate deciduous woodland, thriving in a coastal or near-coastal setting that benefited from maritime climate moderation (West et al., 2021). The Cannonball Seaway, a residual inland sea, likely reduced seasonal extremes and buffered cold snaps, extending the growing season and enhancing climatic stability (West et al., 2021). Such maritime conditions may have further supported high productivity and rich floristic diversity at Ravenscrag (West et al., 2021).

The net primary productivity (NPP) estimates reflect robust forest growth at all three sites, with a decreasing latitudinal trend (Tables 2, 3; West et al., 2021). Some discrepancy in reconstructed NPP may be the result of different methodologies, as West et al. (2021) reconstructed NPP using a transfer function equation based on the average length and width of leaves found in the flora (Li et al., 2020). This univariate approach, although effective in capturing general trends in leaf size–productivity relationships, may overestimate NPP relative to the methods employed herein that incorporate multiple leaf traits and robust datasets from MODIS (Running et al., 2015). Additionally, NPP of the calibration data may be affected by discontinuity of the vegetation at the resolution of the MODIS data (Reichgelt and West, 2025). Taken at face value, the higher NPP values at Ravenscrag may simply reflect favourable growing conditions, such as the buffering of climatic extremes arising from Ravenscrag's coastal proximity.

In general, the NPP values across all three sites indicate a generally productive forest environment, potentially with seasonal cessation of productivity that would have shaped forest composition and structure. The range of reconstructed NPP values for Highvale and Genesee (Tables 2, 3) overlap with the modern NPP of both temperate seasonal forests (824 [631–1049] gC m^{-2} yr^{-1}) and woodlands (585 [358–821] gC m^{-2} yr^{-1}) (Reichgelt and West, 2025), which suggests both Highvale and Genesee may have been a mixed environment sharing qualities of denser temperate seasonal forests and more open woodland environments. That all three sites plot as temperate seasonal forests (Fig. 6) in the Whittaker biome classification system (1962, 1975), fits with the range reflected by our and Ravenscrag NPP estimates (West et al., 2021).

The persistence of waterlogged substrates and saturated soils in the reconstructed swamp and floodplain environments could have further buffered against climatic extremes, sustaining humid microclimates and high evapotranspiration rates even during periods of reduced precipitation. Modern studies on wetlands show that wet to waterlogged habitats exert a moderating effect on temperature and humidity, smoothing intra-annual variability (Krinner, 2003; Hesslerová et al., 2019), which likely would have applied to early Paleocene Alberta. A short but significant dry season, as suggested by the DMP reconstructions and closest climatic analogue affinities (Tables 2, 3, Fig. 7), may have interrupted this general pattern of moisture availability, contributing to seasonal dynamics without fully displacing the overall humid forest environment.

The presence of distinct but related climatic signals between Highvale and Genesee may reflect the differential influence of elevation gradients, shifts in regional precipitation belts, or a latitudinal climate gradient; however, it is also possible that the differences observed are the result of age differences between Highvale and Genesee. Nevertheless, the climate, productivity, and analogue-based reconstructions suggest coherence across a broad regional transect, underscoring the persistence of humid, temperate forest environments in western Canada during the early Paleocene. The compositional overlap between sites, together with evidence for equable climatic conditions from these floras, suggests that the Western Interior of Canada served as a refuge for forest ecosystems during the recovery interval following the K–Pg boundary, supporting the rapid reestablishment of complex, multi-layered vegetation across the region.

CONCLUSIONS

This study documents a diverse early Paleocene macroflora from the Ardley Coal Zone (ACZ) at the Highvale Mine in west-central Alberta, representing one of the few post-K–Pg plant assemblages described in detail from western Canada. The flora includes a fern, a horsetail, two conifers, and 18 broadleaf angiosperms – many of which were probably deciduous. The quantitative palaeoclimate reconstructions using an ensemble framework reveal that Highvale and Genesee both experienced warm-temperate climates with moderate dry seasons and high relative humidity, similar to the nearby Ravenscrag Butte flora of southwestern Saskatchewan (West et al., 2021). Although minor differences in temperature and precipitation are apparent, these may be the result of latitudinal, longitudinal, or elevation differences between the three sites. Despite some variability in reconstructed temperature, precipitation, and productivity, all three sites fall within Whittaker's temperate seasonal forest biome. The reconstructed range net primary productivity values for each site indicate that the sites bordered both temperate seasonal forest and woodland biomes. The Highvale ACZ flora demonstrates that early Paleocene forests in Alberta were compositionally rich and ecologically complex, developing within a mosaic of swamp and floodplain habitats.

ACKNOWLEDGEMENTS

We thank E.B. Koppelhus for access to the University of Alberta Paleobotanical Collection. We thank W.S. Stewart, J.F. Basinger, R.A. Stockey and D.W. Wighton for collecting the specimens, and we thank Bryan Lyons for discussions of mining practices at the Highvale mine at the time of fossil collection. We thank the two anonymous reviewers whose comments improved this manuscript.

ADDITIONAL INFORMATION

CONFLICT OF INTEREST. The authors have declared that no competing interests exist.

ETHICAL STATEMENT. No ethical statement was reported.

FUNDING. No.

REFERENCES

Alvarez, L.W., Alvarez, W., Asaro, F., Michel, H.V., 1980. Extraterrestrial cause for the Cretaceous-Tertiary extinction. Science 208(4448), 1095–1108. https://doi.org/10.1126/science.208.4448.1095

Averyanov, L.V., Phan, K.L., Nguyen, T.H., Nguyen, S.K., Nguyen, T.V., Pham, T.D., 2009. Preliminary observation of native *Glyptostrobus pensilis* (Taxodiaceae) stands in Vietnam. Taiwania 54(3), 191–212.

Barclay, R.S., Johnson, K.R., Betterton, W.J., Dilcher, D.L., 2003. Stratigraphy and megaflora of a K-T boundary section in the eastern Denver Basin, Colorado. Rocky Mountain Geology 38(1), 45–71. https://doi.org/10.2113/gsrocky.38.1.45

Beck, H.E., Zimmermann, N.E., McVicar, T.R., Vergopolan, N., Berg, A., Wood, E.F., 2018. Present and future Köppen-Geiger climate classification maps at 1-km resolution. Scientific Data 5(1), 1–12. https://doi.org/10.1038/sdata.2018.214

Bell, W.A., 1949. Uppermost Cretaceous and Paleocene floras of western Alberta. Geological Survey of Canada Bulletin 13, 1–231. https://doi.org/10.4095/101514

Boulter, M.C., Kvaček, Z., 1989. The Paleocene flora of the Isle of Mull. Palaeontological Association Special Papers in Palaeontology 49, 1–149.

Brown, R.W., 1962. Paleocene flora of the Rocky Mountains and Great Plains. U. S. Geological Survey Professional Paper 375, 1–119. https://doi.org/10.3133/pp375

Budantsev, L.Y., Golovneva, L.B., 2009. Fossil flora of Arctic II – Palaeogene Flora of Spitsbergen. Russian Academy of Sciences, Komarov Botanical Institute, St. Petersburg, 400 pp.

Carvalho, M.R., Jaramillo, C., de la Parra, F., Caballero-Rodríguez, D., Herrera, F., Wing, S., Turner, B.L., D'apolito, C., Romero-Báez, M., Narváez, P., Martínez, C., 2021. Extinction at the end-Cretaceous and the origin of modern Neotropical rainforests. Science 372(6537), 63–68. https://doi.org/10.1126/science.abf1969

Chandrasekharam, A., 1974. Megafossil flora from the Genesee locality, Alberta, Canada. Palaeontographica Abt. B 147, 1–63.

Chaney, R.W., 1951. A revision of fossil *Sequoia* and *Taxodium* in western North America based on the recent discovery of *Metasequoia*. Transactions, American Philosophical Society 40(3), 171–263. https://doi.org/10.2307/1005641

Christophel, D.C., 1976, Fossil floras of the Smoky Tower locality, Alberta, Canada. Palaeontographica Abt. B 157, 1–43.

Crane, P.R., 1981. Studies on the flora of the Reading Beds (Upper Palaeocene). Ph.D. thesis, University of Reading, U.K.

Crane, P.R., Manchester, S.R., Dilcher, D.L., 1988. Morphology and phylogenetic significance of the angiosperm *Platanites hebridicus* from the Palaeocene of Scotland. Palaeontology 31(2), 503–517.

Crane, P.R., Manchester, S.R., Dilcher, D.L., 1991. Reproductive and vegetative structure of *Nordenskioldia* (Trochodendraceae), a vesselless dicotyledon from the early Tertiary of the Northern Hemisphere. American Journal of Botany 78(10), 1311–1334. https://doi.org/10.1002/j.1537-2197.1991.tb12599.x

Davies-Vollum, K.S., 1997. Early Palaeocene palaeoclimatic inferences from fossil floras of the western interior, USA. Palaeogeography, Palaeoclimatology, Palaeoecology 136(1–4), 145–164. https://doi.org/10.1016/S0031-0182(97)00092-8

Demchuk, T.D., 1987. Palynostratigraphy of Paleocene strata of the central Alberta Plains. M.Sc. Thesis, University of Alberta, Edmonton, Alberta, 151 pp.

Demchuk, T.D., 1990. Palynostratigraphic zonation of Paleocene strata in the central and south-central Alberta plains. Canadian Journal of Earth Sciences 27, 1263–1269. https://doi.org/10.1139/e90-136

Demchuk, T.D., 1992. Palynology, petrography and geochemistry of the Ardley coal zone at Wabamun, Alberta. Ph.D. thesis, University of Alberta, Edmonton, Alberta, 321 pp.

Demchuk, T.D., Hills, L.V., 1991. A re-examination of the Paskapoo Formation in the central Alberta Plains: the designation of three new members. Bulletin of Canadian Petroleum Geology 39(3), 270–282. https://doi.org/10.35767/gscpgbull.39.3.270

Demchuk, T., Cameron, A.R., Hills, L.V., 1993. Organic petrology of an early Paleocene coal zone, Wabamun, Alberta: Palynology, petrography and geochemistry. Organic Geochemistry 20(2), 135–148. https://doi.org/10.1016/0146-6380(93)90033-8

Doweld, A.B., 1998. Carpology, seed anatomy, and taxonomic relationships of *Tetracentron* (Tetracentraceae) and *Trochodendron* (Trochodendraceae). Annals of Botany 82(4), 413–443. https://doi.org/10.1006/anbo.1998.0679

Ellis, B., Daly, D.C., Hickey, L.J., Johnson, K.R., Mitchell, J.D., Wilf, P., Wing, S.L., 2009. Manual of leaf architecture. New York Botanical Garden, 190 pp. https://doi.org/10.1079/9781845935849.0000

Fick, S.E., Hijmans, R.J., 2017. WorldClim 2: New 1-km spatial resolution climate surfaces for global land areas. International Journal of Climatology 37(12), 4302–4315. https://doi.org/10.1002/joc.5086

Flynn, A.G., Peppe, D.J., 2019. Early Paleocene tropical forest from the Ojo Alamo Sandstone, San Juan Basin, New Mexico, USA. Paleobiology 45(4), 612–635. https://doi.org/10.1017/pab.2019.24

Forbes, E., 1851. A note on the vegetable remains from Ardtun Head. Quarterly Journal of the Geological Society of London 7, 1–112.

Gibson, D.W., 1977. Sedimentary facies in the Jura-Cretaceous Kootenay Formation, Crowsnest Pass area, southwestern Alberta and southeastern British Columbia. Bulletin of Canadian Petroleum Geology 25(4), 767–791. https://doi.org/10.35767/gscpgbull.27.2.183

Golovneva, L.B., 2002. *Palaeocarpinus* (Betulaceae) from the Paleogene of Spitsbergen and transatlantic floristic migrations. Paleontological Journal 36(4), 422–428.

Golovneva, L.B., Alexeev, P.I., 2017. Taxonomy and morphological diversity of infructescences *Jenkinsella* co-occurred with *Trochodendroides* leaves in the Cretaceous and Paleogene. Palaeobotany 8, 92–121. https://doi.org/10.31111/palaeobotany/2017.8.92

Golovneva, L.B., Zolina, A.A., 2018. Fossil evidence of initial radiation of Cercidiphyllaceae. Palaeobotany 9, 54–75. https://doi.org/10.31111/palaeobotany/2018.9.54

Greenwood, D.R., West, C.K., 2017. A fossil coryphoid palm from the Paleocene of western Canada. Review of Palaeobotany and Palynology 239, 55–65. https://doi.org/10.1016/j.revpalbo.2016.12.002

Greenwood, D.R., Wing, S.L., 1995. Eocene continental climates and latitudinal temperature gradients. Geology 23(11), 1044–1049. https://doi.org/10.1130/0091-7613(1995)023<1044:ECCALT>2.3.CO;2

Heer, O., 1868. Die fossile Flora der Polarländer. Friedrich Schulthess, Zurich, 192 pp.

Heer, O., 1870. Die Miocene Flora und Fauna Spitzbergens. Kongliga Svenska Vetenskaps-Akademiens Handlingar 8(7), 1–98.

Hesslerová, P., Pokorný, J., Huryna, H., Harper, D., 2019. Wetlands and forests regulate climate via evapotranspiration. In: An, S., Verhoven, J. (eds), Wetlands: Ecosystem services, restoration and wise use. Springer, pp. 63–93. https://doi.org/10.1007/978-3-030-14861-4_4

Hickey, L.J., 1977. Stratigraphy and paleobotany of the Golden Valley Formation (Early Tertiary) of western North Dakota. Geological Society of America Memoir 150, 1–183 and 55 plates.

Hijmans, R.J., Cameron, S.E., Parra, J.L., Jones, P.G., Jarvis, A., 2005. Very high resolution interpolated climate surfaces for global land areas. International Journal of Climatology: A Journal of the Royal Meteorological Society 25(15), 1965–1978. https://doi.org/10.1002/joc.1276

Hildebrand, A.R., Penfield, G.T., Kring, D.A., Pilkington, M., Camargo, Z.A., Jacobsen, S.B., Boynton, W.V., 1991. Chicxulub Crater: A possible Cretaceous/Tertiary impact crater on the Yucatán Peninsula, Mexico. Geology 19(9), 867–871. https://doi.org/10.1130/0091-7613(1991)019<0867:CCAPCT>2.3.CO;2

Hoffman, G.L., Stockey, R.A., 1999. Geological setting and paleobotany of the Joffre Bridge Roadcut fossil locality (Late Paleocene), Red Deer Valley, Alberta. Canadian Journal of Earth Sciences 36, 2073–2084. https://doi.org/10.1139/e99-095

Hollick, A., 1936. The Tertiary floras of Alaska, with a chapter on the geology of the Tertiary deposits by Phillip S. Smith. U.S. Geological Survey, Professional Paper 182, 1–185. https://doi.org/10.3133/pp182

Hollis, C.J., Dunkley Jones, T., Anagnostou, E., Bijl, P.K., Cramwinckel, M.J., Cui, Y., Dickens, G.R., Edgar, K.M., Eley, Y., Evans, D., Foster, G.L., 2019. The DeepMIP contribution to PMIP4: Methodologies for selection, compilation and analysis of latest Paleocene and early Eocene climate proxy data, incorporating version 0.1 of the DeepMIP database. Geoscientific Model Development 12(7), 3149–3206. https://doi.org/10.5194/gmd-12-3149-2019

Jerzykiewicz, T., 1997. Stratigraphic framework of the uppermost Cretaceous to Paleocene strata of the Alberta Basin. Geological Survey of Canada, Bulletin 510, 1–121. https://doi.org/10.4095/208902

Jin, B., Tang, L., Lu, Y., Wang, D., Zhang, M., Ma, J., 2012. Temporal and spatial characteristics of male cone development in *Metasequoia glyptostroboides* Hu et Cheng. Plant Signaling & Behavior 7(12), 1687–1694. https://doi.org/10.4161/psb.22898

Johnson, K.R., 1992. Leaf-fossil evidence for extensive floral extinction at the Cretaceous-Tertiary boundary, North Dakota, USA. Cretaceous Research 13(1), 91–117. https://doi.org/10.1016/0195-6671(92)90029-P

Johnson, K.R., 1996. Description of seven common fossil leaf species from the Hell Creek Formation (Upper Cretaceous: Upper Maastrichtian), North Dakota, South Dakota, and Montana. Proceedings of the Denver Museum of Natural History Series 3(12), 1–48.

Johnson, K.R., 2002. Megaflora of the Hell Creek and lower Fort Union Formations in the western Dakotas: Vegetational response to climate change, the Cretaceous-Tertiary boundary event, and rapid marine transgression. In: Hartman, J.H., Johnson, K.R., Nichols, J.D. (eds), The Hell Creek Formation and the Cretaceous-Tertiary boundary in the northern Great Plains: An integrated continental record of the end of the Cretaceous. Geological Society of America Special Paper 361, 329–391. https://doi.org/10.1130/0-8137-2361-2.329

Johnson, K.R., Nichols, Douglas J., Attrep, M., Orth, C.J., 1989. High-resolution leaf-fossil record spanning the Cretaceous/Tertiary boundary. Nature 340(6236), 708–711. https://doi.org/10.1038/340708a0

Koch, B.E., 1963. Fossil plants from the lower Paleocene of the Agatdalen (Angmartussut) area, central Nugssuaq Peninsula, northwest Greenland. Grønslands Geologiske Undersøgelse Bulletin 38, 1–120. https://doi.org/10.34194/bullggu.v38.6572

Krinner, G., 2003. Impact of lakes and wetlands on boreal climate. Journal of Geophysical Research: Atmospheres 108(D16), 1–18. https://doi.org/10.1029/2002JD002597

Kvaček, Z., Manum, S.B., Boulter, M.C., 1994. Angiosperms from the Palaeogene of Spitsbergen, including an unfinished work by AG Nathorst. Palaeontographica Abt. B 232, 103–128.

Langenberg, C.W., Berhane, H., Sweet, A.R., Marchioni, D., Heaman, L.M., 2007. Regional Correlations of the Ardley Coal Zone. Alberta, EUB/AGS Earth Science Report 5, 21 pp.

LePage, B.A., 2007. The taxonomy and biogeographic history of *Glyptostrobus* Endlicher (Cupressaceae). Bulletin of the Peabody Museum of Natural History 48(2), 359–426. https://doi.org/10.3374/0079-032X(2007)48[359:TTABHO]2.0.CO;2

LePage, B.A., Yang, H., Matsumoto, M., 2005. The Evolution and Biogeographic History of *Metasequoia*. In: LePage, B.A., Williams, C.J., Yang, H. (eds) The Geobiology and Ecology of *Metasequoia*. Topics in Geobiology, vol 22. Springer, Dordrecht, pp. 3–114 https://doi.org/10.1007/1-4020-2764-8_1

Li, Y., Reich, P.B., Schmid, B., Shrestha, N., Feng, X., Lyu, T., Maitner, B.S., Xu, X., Li, Y., Zou, D., Zheng-Hong, T. Xiangyan, S., Tang, Z., Guo, Q., Feng, X. Enquist, B.J., Wang, Z., 2020. Leaf size woody dicots predicts ecosystem primary productivity. Ecology Letters 23(6), 1003–1013. https://doi.org/10.1111/ele.13503

Liu, Y.J., Li, C.S., Wang, Y.F., 1999. Studies on fossil *Metasequoia* from north-east China and their taxonomic implications. Botanical Journal of the Linnean Society 130(3), 267–297. https://doi.org/10.1111/j.1095-8339.1999.tb00523.x

Lowe, A.J., Greenwood, D.R., West, C.K., Galloway, J.M., Sudermann, M., Reichgelt, T., 2018. Plant community ecology and climate on an upland volcanic landscape during the Early Eocene Climatic Optimum: McAbee Fossil Beds, British Columbia, Canada. Palaeogeography, Palaeoclimatology, Palaeoecology 511, 433–448. https://doi.org/10.1016/j.palaeo.2018.09.010

Manchester, S.R., 1999. Biogeographical relationships of North American Tertiary floras. Annals of the Missouri Botanical Garden 86(2), 472–522. https://doi.org/10.2307/2666183

Manchester, S.R., 2014. Revisions to Roland Brown's North American Paleocene flora. Acta Musei Nationalis Pragae Series B-Historia Naturalis 70(3–4), 153–210.

Manchester, S.R., 2025. *Tetracentron* (Trochodendraceae) in the Paleocene and Miocene of western North America. Journal of Plant Research 138, 555–561. https://doi.org/10.1007/s10265-025-01636-6

Manchester, S.R., Hickey, L.J., 2007. Reproductive and vegetative organs of *Browniea* gen. n. (Nyssaceae) from the Paleocene of North America. International Journal of Plant Sciences 168(2), 229–249. https://doi.org/10.1086/509661

Manchester, S.R., Pigg, K.P., Devore, M.L., 2018. Trochodendraceous fruits and foliage in the Miocenc of western North America. Acta Musei Nationalis Pragae Series B-Historia Naturalis 74(1–2), 45–54. https://doi.org/10.2478/if-2018-0004

Manchester, S.R., Foster, A., Lott, T.A., 2023. The Paleocene Horse Creek florule, Tongue River Member of the Fort Union Formation, southeastern Montana, USA. Acta Palaeobotanica 63(1), 32–53. https://doi.org/10.35535/acpa-2023-0003

McIver, E.E., Basinger, J.F., 1993. Flora of the Ravenscrag Formation (Paleocene), Southwestern Saskatchewan, Canada. Palaeontographica Canadiana 10, 1–167.

Miller Jr., C.N., 1967. Evolution of the fern genus *Osmunda*. Contributions from the Museum of Paleontology, University of Michigan 21(8), 139–203.

Moiseeva, M.G., Kodrul, T.M., Herman, A.B., 2018. Early Paleogene Boguchan flora of the Amur Region (Russian Far East): Composition, age and palaeoclimatic implications. Review of Palaeobotany and Palynology 253, 15–36. https://doi.org/10.1016/j.revpalbo.2018.03.003

Morgan, J.V., Bralower, T.J., Brugger, J., Wünnemann, K., 2022. The Chicxulub impact and its environmental consequences. Nature Reviews Earth and Environment 3(5), 338–354. https://doi.org/10.1038/s43017-022-00283-y

Nares, F.R., Huegele, I.B., Manchester, S.R., 2025. Compound-leaved Platanaceae in the Eocene of western North America. International Journal of Plant Sciences 186(1), 68–79. https://doi.org/10.1086/732310

Newberry, J.S., 1868. Notes on the later extinct floras of North America. Annals of the Lyceum of Natural History of New York 9, 1–76.

Nichols, D.J., Ott, H.L., 1978. Biostratigraphy and evolution of the *Momipites*–*Caryapollenites* lineage in the early Tertiary in the Wind River Basin, Wyoming. Palynology 2(1), 93–112. https://doi.org/10.1080/01916122.1978.9989167

Nichols, D.J., Johnson, K.R., 2002. Palynology and microstratigraphy of Cretaceous–Tertiary boundary sections in southwestern North Dakota. In: Hartman, J.H., Johnson, K.R., Nichols, D.J. (eds), The Hell Creek Formation and the Cretaceous-Tertiary Boundary in the northern Great Plains: An integrated continental record of the end of the Cretaceous. Geological Society of America Special Paper 361, 95–143. https://doi.org/10.1130/0-8137-2361-2.75

Nichols, D.J., Jarzen, D.M., Orth, C.J., Oliver, P.Q., 1986. Palynological and iridium anomalies at Cretaceous-Tertiary boundary, south-central Saskatchewan. Science 231(4739), 714–717. https://doi.org/10.1126/science.231.4739.714

Oksanen, J., Simpson, G., Blanchet, F., Kindt, R., Legendre, P., Minchin, P., O'Hara, R., Solymos, P., Stevens, M., Szoecs, E., Wagner, H., Barbour, M., Bedward, M., Bolker, B., Borcard, D., Carvalho, G., Chirico, M., De Caceres, M., Durand S., Evangelista, H., FitzJohn, R., Friendly, M., Furneaux, B., Hannigan, G., Hill, M., Lahti, L., McGlinn, D., Ouellette, M., Ribeiro Cunha, E., Smith, T., Stier, A., Ter Braak, C., Weedon, J., Borman, T., 2025. vegan: Community Ecology Package. R package version 2.6-10. Available from https://CRAN.R-project.org.package-vegan. Accessed September 2025.

Orth, C.J., Gilmore, J.S., Knight, J.D., Pillmore, C.L., Tschudy, R.H., Fassett, J.E., 1981. An iridium abundance anomaly at the palynological Cretaceous-Tertiary boundary in northern New Mexico. Science 214(4527), 1341–1343. https://doi.org/10.1126/science.214.4527.1341

Parrish, J.T., Spicer, R.A., 1988. Late Cretaceous terrestrial vegetation: a near-polar temperature curve. Geology 16(1), 22–25. https://doi.org/10.1130/0091-7613(1988)016<0022:LCTVAN>2.3.CO;2

Pearce, C.M., Cordes, L.D., 1988. The distribution and ecology of water horsetail (*Equisetum fluviatile*) in northern wetlands. Journal of Freshwater Ecology 4(3), 383–394. https://doi.org/10.1080/02705060.1988.9665187

Penhallow, D.P., 1908. Report on Tertiary plants of British Columbia collected by Lawrence M. Lambe in 1906 together with a discussion of previously recorded Tertiary floras. Canada Department of

Mines, Geological Survey Branch, No. 1013, 167 pp. https://doi.org/10.4095/106549

Peppe, D.J., 2009. A high resolution chronostratigraphic study of the early Paleocene floral record in the northern Great Plains. Ph.D. thesis, Yale University, New Haven, 590 pp.

Prebble, J.G., Kennedy, E.M., Reichgelt, T., Clowes, C., Womack, T., Mildenhall, D.C., Raine, J.I., Crouch, E.M., 2021. A 100 million year composite pollen record from New Zealand shows maximum angiosperm abundance delayed until Eocene. Palaeogeography, Palaeoclimatology, Palaeoecology 556, e110207. https://doi.org/10.1016/j.palaeo.2020.110207

R Core Team, 2024. R: A language and environment for statistical computing. Vienna R Foundation for Statistical Computing, Vienna, Austria. Available from: https://www.R-project.org/. Accessed September 2025.

Reichgelt, T., West, C.K., 2025. Insights into greener Miocene biomes and globally enhanced terrestrial productivity from fossil leaves. Evolving Earth 3(1), 100058. https://doi.org/10.1016/j.eve.2025.100058

Reichgelt, T., Greenwood, D.R., Steinig, S., Conran, J.G., Hutchinson, D.K., Lunt, D.J., Scriven, L.J., Zhu, J., 2022. Plant proxy evidence for high rainfall and productivity in the Eocene of Australia. Paleoceanography and Paleoclimatology 37(6), 2022PA004418. https://doi.org/10.1029/2022PA004418

Retallack, G.J., 1997. Dinosaurs and dirt. In: Soil Grown Tall: The Epic Saga of Life from Earth, 113–123. https://doi.org/10.1007/978-3-030-88739-1_8

Richardson, R.J.H., Strobl, R.S., MacDonald, D.E., Nurkowski, J.R., McCabe, P.J., Bosman, A., 1988. An evaluation of coal resources of the Ardley coal zone to a depth of 400 m in the Alberta Plains area. Alberta Research Council, Open File Report 1988-02, 85 pp.

Rosenberg, Y.O., Ashckenazi-Polivoda, S., Abramovich, S., Thibault, N., Chin, S., Feinstein, S., Bartov, Y., Amrani, A., 2021. Resilience of primary and export productivity in a eutrophic ecosystem following the Cretaceous-Paleogene mass extinction. Global and Planetary Change 196, 103371. https://doi.org/10.1016/j.gloplacha.2020.103371

Royer, D.L., Meyerson, L.A., Robertson, K.M., Adams, J.M., 2009. Phenotypic plasticity of leaf shape along a temperature gradient in *Acer rubrum*. PloS One 4(10), e7653. https://doi.org/10.1371/journal.pone.0007653

Running, S.W., Mu, Q., Zhao, M., 2015. MOD17A3H MODIS/terra net primary production yearly L4 global 500m SIN grid V006. NASA EOSDIS Land Processes Distributed Active Archive Center. https://doi.org/10.5067/MODIS/MOD17A3H.006

Russell, D.A., Singh, C., 1978. The Cretaceous–Tertiary boundary in south-central Alberta – a reappraisal based on dinosaurian and microfloral extinctions. Canadian Journal of Earth Sciences 15(2), 284–292. https://doi.org/10.1139/e78-029

Schneider, C.A., Rasband, W.S., Eliceiri, K.W., 2012. NIH Image to ImageJ: 25 years of image analysis. Nature Methods 9(7), 671–675. https://doi.org/10.1038/nmeth.2089

Schulte, P., Alegret, L., Arenillas, I., Arz, J.A., Barton, P.J., Bown, P.R., Bralower, T.J., Christeson, G.L., Claeys, P., Cockell, C.S., Collins, G.S., 2010. The Chicxulub asteroid impact and mass extinction at the Cretaceous-Paleogene boundary. Science 327(5970), 1214–1218. https://doi.org/10.1126/science.1177265

Spicer, R.A., 2008. Frontiers in palaeobotany: Plant fossils and their role in predicting future climate change. Journal of Palaeosciences 57(1–3), 415–427. https://doi.org/10.54991/jop.2008.257

Spicer, R.A., Yang, J., Spicer, T.E., Farnsworth, A., 2021. Woody dicot leaf traits as a palaeoclimate proxy: 100 years of development and application. Palaeogeography, Palaeoclimatology, Palaeoecology 562, 110138. https://doi.org/10.1016/j.palaeo.2020.110138

Ştefan, V., Levin, S., 2018. Plotbiomes: R package for plotting Whittaker biomes with ggplot2 (v1.0.0). Zenodo. https://doi.org/10.5281/zenodo.7145245

Stiles, E., Wilf, P., Iglesias, A., Gandolfo, M.A., Cúneo, N.R., 2020. Cretaceous–Paleogene plant extinction and recovery in Patagonia. Paleobiology 46(4), 445–469. https://doi.org/10.1017/pab.2020.45

Stockey, R.A., Rothwell, G.W., Falder, A.B., 2001. Diversity among taxodioid conifers: *Metasequoia foxii* sp. nov. from the Paleocene of central Alberta, Canada. International Journal of Plant Sciences 162(1), 221–234. https://doi.org/10.1086/317914

Stockey, R.A., Hoffman, G.L., Vavrek, M.J., 2014. Paleobotany and paleoecology of the Munce's Hill fossil locality near Red Deer, Alberta, Canada. In: Stevens, W.D., Montiel, O.M., Raven, P.H. (eds), Paleobotany and Biogeography: A Festschrift for Alan Graham in His 80th Year. Missouri Botanical Gardens Monograph 128, 367–388.

Sun, F., Stockey, R.A., 1992. A new sepcies of *Palaeocarpinus* (Betulaceae) based on infructescences, fruits, and associated staminate inflorescences and leaves from the Paleocene of Alberta, Canada. International Journal of Plant Sciences 153(1), 136–146. https://doi.org/10.1086/297015

Sweet, A.R., 1986. The Cretaceous–Tertiary boundary in the central Alberta Foothills. II: Miospore and pollen taxonomy. Canadian Journal of Earth Sciences 23(9), 1375–1388. https://doi.org/10.1139/e86-131

Sweet, A.R., Braman, D.R., 2001. Cretaceous–Tertiary palynofloral perturbations and extinctions within the *Aquilapollenites* phytogeographic province. Canadian Journal of Earth Sciences 38(2), 249–269. https://doi.org/10.1139/e00-024

Sweet, A.R., Braman, D.R., Lerbekmo, J.F., 1990. Palynofloral response to K/T boundary events: a transitory interruption within a dynamic system. In: Sharpton, V.L., Ward, P.D. (eds), Global Catastrophes in Earth History: An Interdisciplinary

Conference on Impacts, Volcanism, and Mass Mortality. Geological Society of America Special Paper 247, 457–469. https://doi.org/10.1130/SPE247-p457

Vajda, V., Bercovici, A., 2014. The global vegetation pattern across the Cretaceous–Paleogene mass extinction interval: a template for other extinction events. Global and Planetary Change 122, 29–49. https://doi.org/10.1016/j.gloplacha.2014.07.014

Vellekoop, J., Sluijs, A., Smit, J., Schouten, S., Weijers, J.W., Sinninghe Damsté, J.S., Brinkhuis, H., 2014. Rapid short-term cooling following the Chicxulub impact at the Cretaceous–Paleogene boundary. Proceedings of the National Academy of Sciences 111(21), 7537–7541. https://doi.org/10.1073/pnas.1319253111

Vellekoop, J., Kaskes, P., Smit, J., Speijer, R., Claeys, P., 2021. Rapid biological recovery following the Cretaceous-Paleogene boundary catastrophe in the Maastrichtian type area. Geological Society of America Abstracts with Programs 53(6), 12–13. https://doi.org/10.1130/abs/2021AM-371444

West, C.K., Greenwood, D.R., Basinger, J.F., 2015. Was the Arctic Eocene 'rainforest' monsoonal? Estimates of seasonal precipitation from early Eocene megafloras from Ellesmere Island, Nunavut. Earth and Planetary Science Letters 427, 18–30. https://doi.org/10.1016/j.epsl.2015.06.036

West, C.K., Greenwood, D.R., Basinger, J.F., 2019. The late Paleocene to early Eocene Arctic megaflora of Ellesmere and Axel Heiberg islands, Nunavut, Canada; The late Paleocene to early Eocene Arctic megaflora of Ellesmere and Axel Heiberg islands, Nunavut, Canada. Palaeontographica Abt. B 300(1–6), 47–163. https://doi.org/10.1127/palb/2019/0066

West, C.K., Greenwood, D.R., Reichgelt, T., Lowe, A.J., Vachon, J.M., Basinger, J.F., 2020. Paleobotanical proxies for early Eocene climates and ecosystems in northern North America from middle to high latitudes. Climate of the Past 16(4), 1387–1410. https://doi.org/10.5194/cp-16-1387-2020

West, C.K., Reichgelt, T., Basinger, J.F., 2021. The Ravenscrag Butte flora: Paleoclimate and paleoecology of an early Paleocene (Danian) warm-temperate deciduous forest near the vanishing inland Cannonball Seaway. Palaeogeography, Palaeoclimatology, Palaeoecology 576, 110488. https://doi.org/10.1016/j.palaeo.2021.110488

West, C.K., Reichgelt, T., Reyes, A.V., Buryak, S.D., Staniszewska, K.J., Basinger, J.F., 2024. Paleobotanical evidence for Mediterranean climates in the western Canadian paleoarctic during the late middle Eocene. Paleoceanography and Paleoclimatology 39(10), p.e2024PA004874. https://doi.org/10.1029/2024PA004874

Whittaker, R.H., 1962. Classification of natural communities. Botanical Review 28(1), 1–239. https://doi.org/10.1007/BF02860872

Whittaker, R.H., 1975. Communities and Ecosystems, 2nd ed. MacMillan Publishing, New York.

Wilf, P., 1997. When are leaves good thermometers? A new case for leaf margin analysis. Paleobiology 23(3), 373–390. https://doi.org/10.1017/S0094837300019746

Wilf, P., Johnson, K.R., 2004. Land plant extinction at the end of the Cretaceous: a quantitative analysis of the North Dakota megafloral record. Paleobiology 30(3), 347–368. https://doi.org/10.1666/0094-8373(2004)030<0347:LPEATE>2.0.CO;2

Wilf, P., Wing, S.L., Greenwood, D.R., Greenwood, C.L., 1998. Using fossil leaves as paleoprecipitation indicators: An Eocene example. Geology 26(3), 203–206. https://doi.org/10.1130/0091-7613(1998)026<0203:UFLAPI>CO;2

Wilf, P., Carvalho, M.R., Stiles, E., 2023. The end-Cretaceous plant extinction: heterogeneity, ecosystem transformation, and insights for the future. Cambridge Prisms: Extinction 1, e14. https://doi.org/10.1017/ext.2023.13

Willard, D.A., Donders, T.H., Reichgelt, T., Greenwood, D.R., Sangiorgi, F., Peterse, F., Nierop, K.G., Frieling, J., Schouten, S., Sluijs, A., 2019. Arctic vegetation, temperature, and hydrology during Early Eocene transient global warming events. Global and Planetary Change 178, 139–152. https://doi.org/10.1016/j.gloplacha.2019.04.012

Wilson Deibel, P.K., Wilson Mantilla, G.P., Strömberg, C.A.E, 2024. Plant taxonomic turnover and diversity across the Cretaceous/Paleogene boundary in northeastern Montana. Paleobiology 50(4), 608–626. https://doi.org/10.1017/pab.2024.22

Wing, S.L., Greenwood, D.R., 1993. Fossils and fossil climate: the case for equable continental interiors in the Eocene. Philosophical Transactions of the Royal Society of London, Series B, Biological Sciences 341(1297), 243–252. https://doi.org/10.1098/rstb.1993.0109

Wolfe, J.A., 1966. Tertiary plants from the Cook Inlet region, Alaska. U. S. Geological Survey Professional Paper 398-B, 1–32. https://doi.org/10.3133/pp398B

Wolfe, J.A., 1993. A method of obtaining climatic parameters from leaf assemblages. U. S. Geological Survey Bulletin 2040, 1–71. https://doi.org/10.3133/b2040

Wolfe, J.A., Upchurch, G.R., 1986. Vegetation, climatic and floral changes at the Cretaceous-Tertiary boundary. Nature 324(6093), 148–152. https://doi.org/10.1038/324148a0

Wolfe, J.A., Upchurch Jr., G.R., 1987. Leaf assemblages across the Cretaceous-Tertiary boundary in the Raton Basin, New Mexico and Colorado. Proceedings of the National Academy of Sciences 84(15), 5096–5100. https://doi.org/10.1073/pnas.84.15.5096

Yang, J., Spicer, R.A., Spicer, T.E., Li, C.S., 2011. 'CLAMP Online': a new web-based palaeoclimate tool and its application to the terrestrial Paleogene and Neogene of North America. Palaeobiodiversity and Palaeoenvironments 91, 163–183. https://doi.org/10.1007/s12549-011-0056-2

Yang, J., Spicer, R.A., Spicer, T.E., Arens, N.C., Jacques, F.M., Su, T., Kennedy, E.M., Herman, A.B., Steart, D.C., Srivastava, G., Mehrotra, R.C., 2015. Leaf form–climate relationships on the global stage: an ensemble of characters. Global Ecology and Biogeography 24(10), 1113–1125. https://doi.org/10.1111/geb.12334

Zhang, L., Hay, W.W., Wang, C., Gu, X., 2019. The evolution of latitudinal temperature gradients from the latest Cretaceous through the Present. Earth-Science Reviews 189, 147–158. https://doi.org/10.1016/j.earscirev.2019.01.025

Zolina, A.A., Manchester, S.R., Golovneva, L.B., 2021. Typification of the genus *Zizyphoides* Seward et Conway (Magnoliophyta, Trochodendraceae). Acta Palaeobotanica 61(2), 123–135. https://doi.org/10.35535/acpa-2021-0007